Commun. Comput. Phys.
doi: 10.4208/cicp.OA-2018-0104

Vol. **25**, No. 5, pp. 1496-1522
May 2019

Error Analysis of the Plane Wave Discontinuous Galerkin Method for Maxwell's Equations in Anisotropic Media

Long Yuan[1] and Qiya Hu[2,3,*]

[1] *College of Mathematics and Systems Science, Shandong University of Science and Technology, Qingdao 266590, China.*
[2] *LSEC, Institute of Computational Mathematics and Scientic/Engineering Computing, Academy of Mathematics and Systems Science, Chinese Academy of Sciences, Beijing 100190, China.*
[3] *School of Mathematical Sciences, University of Chinese Academy of Sciences, Beijing 100049, China.*

Received 16 April 2018; Accepted (in revised version) 21 June 2018

Abstract. In this paper we investigate the plane wave discontinuous Galerkin method for three-dimensional anisotropic time-harmonic Maxwell's equations with diagonal matrix coefficients. By introducing suitable transformations, we define new plane wave basis functions and derive error estimates of the approximate solutions generated by the proposed discretization method for the considered homogeneous equations. In the error estimates, some dependence of the error bounds on the condition number of the coefficient matrix is explicitly given. Combined with local spectral element method, we further prove a convergence result for the nonhomogeneous case. Numerical results verify the validity of the theoretical results, and indicate that the resulting approximate solutions generated by the PWDG possess high accuracies.

AMS subject classifications: 65N30, 65N55

Key words: Time-harmonic Maxwell's equations, anisotropic media, plane-wave basis, error estimates, nonhomogeneous.

1 Introduction

The plane-wave method falls into the class of Trefftz methods [27], which has recently been systematically surveyed in [9]. The plane-wave method was first introduced to solve Helmholtz equation and was then extended to solve time-harmonic Maxwell's equations and elastic wave equations. Examples of this approach include the variational

*Corresponding author. *Email addresses:* `yuanlong@lsec.cc.ac.cn` (L. Yuan), `hqy@lsec.cc.ac.cn` (Q. Hu)

theory of complex rays (VTCR) [23, 24], the ultra weak variational formulation (UWVF) [2–5, 14–17, 31, 33], the plane-wave discontinuous Galerkin (PWDG) method [6–8, 30], the plane-wave least-squares (PWLS) method [10, 11, 22, 29, 32, 34] and the plane-wave least-squares combined with local spectral finite element (PWLS-LSFE) method [12,13]. Today, there are other dedicated computational strategies for the resolution of wave equations (see [1, 19, 28]).

Recently, the UWVF method was extended to solve homogeneous Maxwell's equations in anisotropic media [15]. The studies in [15] were devoted to approximating the Robin-type trace of the electric and magnetic fields in an anisotropic medium, and focus on the numerical tests and convergence analysis in TM mode scattering, which can result in a Helmholtz equation in two dimensions with an anisotropic coefficient.

For the three-dimensional anisotropic time-harmonic Maxwell's system, it was pointed out in [15, p.351] that *almost all theoretical questions related to the 3D UWVF approach to anisotropic media are still open: in particular, the revelent approximation properties of sums of anisotropic plane waves are not known* . To our knowledge, the other plane wave methods have not been generalized to solve the three-dimensional anisotropic Maxwell's equations. The existing numerical results indicate that the PWDG method can generate approximate solutions with higher accuracies.

In this paper we are mainly interested in extension of the PWDG method to the three-dimensional time-harmonic Maxwell's equations in anisotropic media (with diagonal matrix coefficients). Motivated by the results in [25], the permittivity ε and the permeability μ are assumed to be of the form

$$\begin{aligned} \varepsilon &= \varepsilon_r \mathrm{diag}(a_x, a_y, a_z) = \varepsilon_r\, \Lambda, \\ \mu &= \mu_r \mathrm{diag}(a_x, a_y, a_z) = \mu_r\, \Lambda, \end{aligned} \tag{1.1}$$

where the diagonal matrix $\Lambda = \mathrm{diag}(a_x, a_y, a_z)$, $\varepsilon_r, \mu_r, a_x, a_y$ and a_z are constant. Example electromagnetic problems within this class include the design of waveguides and antennas, scattering of electromagnetic waves from automobiles and aircraft, and the penetration and absorption of electromagnetic waves by dielectric objects. Under this assumption, a permittivity, ε, and permeability, μ, tensor can describe a linear metamaterial with no magnetoelectric coupling, where Bianisotropy effects have typically played a minor role in the overall response of the experimental metamaterials, and can be mitigated by design (see [18]).

In this paper, we propose a scaling transformation and a coordinate transformation and verify some stabilities of the two transformations. Based on these, we define new plane wave basis functions associated with the considered model and derive error estimates of the approximate solutions generated by the PWDG for the underlying Maxwell's equations. Moreover, by combining the ideas in [12] we apply the proposed method to solve anisotropic nonhomogeneous Maxwell's equations and derive the corresponding error estimates. The theoretical results show that the errors of the resulting approximate solutions are affected by the condition number of the anisotropic coefficient matrix in Maxwell's equations. We can also extend the results to the PWLS method for the considered model.

Numerical experiments indicate that the approximate solutions generated by the proposed PWDG method possess high accuracy, and verify the validity of the theoretical results. Moreover, the approximate solution generated by the PWDG method is slightly more accurate than that generated by the PWLS method for the homogeneous case.

The paper is organized as follows: In Section 2, we recall the Maxwell boundary value problem. In Section 3, we describe the proposed PWDG method for the three-dimensional homogeneous Maxwell's equations in anisotropic media associated with triangulation. In Section 4, we explain how to discretize the variational problem. In Section 5, we derive error estimates for the corresponding approximate solutions. In Section 6, a PWDG-LSFE method is presented for nonhomogeneous Maxwell equations. Finally, we report some numerical results to confirm the effectiveness of the proposed method.

2 The Maxwell boundary value problem

In this section we recall the first-order system of time-harmonic Maxwell's equations. Then, by the transformation, we derive the corresponding vector Helmholtz equations.

The considered problem is based on a partition of the solution domain. Let Ω be the underlying domain in $\mathbf{R}^3$. For convenience, assume that Ω is a bounded polyhedron. Let Ω be divided into the union of some subdomains in the sense that

$$\overline{\Omega}=\bigcup_{k=1}^{N}\overline{\Omega}_k,\quad \Omega_l\bigcap\Omega_j=\emptyset,\quad \text{for } l\neq j,$$

where each Ω_k is a polyhedron. Let $\mathcal{T}_h$ denote the partition comprised of the elements $\{\Omega_k\}$, where h is the mesh width of the triangulation. As usual, we assume that $\mathcal{T}_h$ is quasi-uniform. Define

$$\Gamma_{lj}=\partial\Omega_l\bigcap\partial\Omega_j,\quad \text{for } l\neq j$$

and

$$\gamma_k=\overline{\Omega}_k\bigcap\partial\Omega\quad (k=1,\cdots,N),\quad \gamma=\bigcup_{k=1}^{N}\gamma_k.$$

We denote by $\mathcal{F}_h=\bigcup_k\partial\Omega_k$ the skeleton of the mesh, and set $\mathcal{F}_h^{\mathrm{B}}=\mathcal{F}_h\bigcap\partial\Omega$ and $\mathcal{F}_h^{\mathrm{I}}=\mathcal{F}_h\backslash\mathcal{F}_h^{\mathrm{B}}$. Let u and σ be a piecewise smooth function and vector field on $\mathcal{T}_h$, respectively. On $\partial\Omega_l\bigcap\partial\Omega_j$, we define

$$\begin{aligned}&\text{the averages: } \{\{u\}\}:=\frac{u_l+u_j}{2},\quad \{\{\sigma\}\}:=\frac{\sigma_l+\sigma_j}{2},\\ &\text{the jumps: } [\![\sigma]\!]_T:=\mathbf{n}_l\times\sigma_l+\mathbf{n}_j\times\sigma_j,\quad [\![\sigma]\!]_N=\mathbf{n}_l\cdot\sigma_l+\mathbf{n}_j\cdot\sigma_j,\end{aligned}\tag{2.1}$$

where $\mathbf{n}$ denotes a unit outer normal vector on the boundary of each element Ω_k.

We want to compute a numerical approximation of the electromagnetic field $(\mathbf{E}, \mathbf{H})$ solution of the three-dimensional (3D) time-harmonic homogeneous Maxwell equations written as a first-order system of equations:

$$\begin{cases} \nabla\times\mathbf{E}-i\omega\mu\mathbf{H}=\mathbf{0}, \\ \nabla\times\mathbf{H}+i\omega\varepsilon\mathbf{E}=\mathbf{0}, \\ \nabla\cdot(\varepsilon\cdot\mathbf{E})=0, \\ \nabla\cdot(\mu\cdot\mathbf{H})=0, \end{cases} \quad \text{in } \Omega, \tag{2.2}$$

with the lowest-order absorbing boundary condition

$$\mathbf{H}\times\mathbf{n}-\vartheta(\mathbf{n}\times\mathbf{E})\times\mathbf{n}=\mathbf{g}/i\omega \quad \text{on} \quad \gamma=\partial\Omega. \tag{2.3}$$

Here, $\mathbf{E}=(E_x,E_y,E_z)^T$, $\mathbf{H}=(H_x,H_y,H_z)^T$, and the superscript T denotes matrix transposition. $\omega>0$ is the temporal frequency of the field, $\vartheta\neq0$ is assumed to be constant, and $\mathbf{g}\in L^2_{\mathbf{T}}(\partial\Omega)$. The permittivity $\varepsilon(\mathbf{x})$ and the permeability $\mu(\mathbf{x})$ are assumed to be real strictly positive definite matrices. All material coefficients are assumed to be constant in the whole domain.

Define the scaled fields $\tilde{\mathbf{E}}$ and $\tilde{\mathbf{H}}$ as follows:

$$\begin{aligned} &(\tilde{E}_x,\tilde{E}_y,\tilde{E}_z)^T=G^{-1}(E_x,E_y,E_z)^T, \\ &(\tilde{H}_x,\tilde{H}_y,\tilde{H}_z)^T=G^{-1}(H_x,H_y,H_z)^T. \end{aligned} \tag{2.4}$$

Here the elements of the diagonal matrix $G=\text{diag}\{g_x,g_y,g_z\}$ are real strictly positive constants and will be given later. Using (1.1) and (2.4), the original Maxwell equations can be written in terms of the scaled fields $\tilde{\mathbf{E}}$ and $\tilde{\mathbf{H}}$:

$$\begin{aligned} &\nabla\times(G\tilde{\mathbf{E}})-i\omega\mu_r\Lambda G\tilde{\mathbf{H}}=\mathbf{0}, \\ &\nabla\times(G\tilde{\mathbf{H}})+i\omega\varepsilon_r\Lambda G\tilde{\mathbf{E}}=\mathbf{0}, \\ &\nabla\cdot(\varepsilon_r\Lambda G\tilde{\mathbf{E}})=0, \\ &\nabla\cdot(\mu_r\Lambda G\tilde{\mathbf{H}})=0. \end{aligned} \tag{2.5}$$

A suitable choice of the scaling factors g_x,g_y,g_z according to the equations

$$\frac{g_x}{g_y}=\sqrt{\frac{a_y}{a_x}}, \quad \frac{g_y}{g_z}=\sqrt{\frac{a_z}{a_y}} \quad \text{and} \quad \frac{g_z}{g_x}=\sqrt{\frac{a_x}{a_z}} \tag{2.6}$$

allows us to transform the system of (2.5) into the following form

$$\begin{aligned} &\nabla_{\mathbf{a}}\times\tilde{\mathbf{E}}-i\omega\mu_r\tilde{\mathbf{H}}=\mathbf{0}, \\ &\nabla_{\mathbf{a}}\times\tilde{\mathbf{H}}+i\omega\varepsilon_r\tilde{\mathbf{E}}=\mathbf{0}, \\ &\nabla_{\mathbf{a}}\cdot(\varepsilon_r\tilde{\mathbf{E}})=0, \\ &\nabla_{\mathbf{a}}\cdot(\mu_r\tilde{\mathbf{H}})=0, \end{aligned} \tag{2.7}$$

where

$$\nabla_{\mathbf{a}} \overset{\text{def}}{=\!=} \mathbf{i}\frac{1}{\sqrt{a_y a_z}}\partial_x + \mathbf{j}\frac{1}{\sqrt{a_z a_x}}\partial_y + \mathbf{k}\frac{1}{\sqrt{a_x a_y}}\partial_z, \quad \Lambda G = \sqrt{a_x}\Lambda^{1/2}$$

and

$$\begin{cases} \nabla\times(G\tilde{\mathbf{E}}) = \sqrt{a_x}\Lambda^{1/2}\nabla_{\mathbf{a}}\times\tilde{\mathbf{E}}, \\ \nabla\times(G\tilde{\mathbf{H}}) = \sqrt{a_x}\Lambda^{1/2}\nabla_{\mathbf{a}}\times\tilde{\mathbf{H}}. \end{cases} \tag{2.8}$$

Here, $\mathbf{i}$,$\mathbf{j}$ and $\mathbf{k}$ are the standard unit vectors in $\mathbf{R}^3$. By (2.6), we can obtain

$$g_x = 1, \quad g_y = \sqrt{\frac{a_x}{a_y}} \quad \text{and} \quad g_z = \sqrt{\frac{a_x}{a_z}}.$$

Set

$$s_x = \sqrt{a_y a_z}, \quad s_y = \sqrt{a_z a_x} \quad \text{and} \quad s_z = \sqrt{a_x a_y}.$$

Define the coordinate transformation

$$\hat{\mathbf{x}} = (\hat{x},\hat{y},\hat{z})^T = \text{diag}(s_x,s_y,s_z)\,(x,y,z)^T \overset{\Delta}{=\!=} M\,(x,y,z)^T \overset{\Delta}{=\!=} M\,\mathbf{x}. \tag{2.9}$$

Under the coordinate transformation (2.9), we assume that the element $\Omega_k \in \mathcal{T}_h$ is transformed into the element $\hat{\Omega}_k$. Let $\hat{\mathcal{T}}_{\hat{h}}$ denote the partition comprising the elements $\{\hat{\Omega}_k\}$, where $\hat{h}$ is the mesh width of the transformed partition. Set $\hat{\mathcal{F}}_{\hat{h}} = \bigcup_k \partial\hat{\Omega}_k$, $\hat{\mathcal{F}}^{\mathrm{B}}_{\hat{h}} = \partial\hat{\Omega}$ and $\hat{\mathcal{F}}^{\mathrm{I}}_{\hat{h}} = \hat{\mathcal{F}}_{\hat{h}} \backslash \hat{\mathcal{F}}^{\mathrm{B}}_{\hat{h}}$.

Then the scaled electric and magnetic fields $(\hat{\mathbf{E}}(\hat{\mathbf{x}}),\hat{\mathbf{H}}(\hat{\mathbf{x}})) = (\tilde{\mathbf{E}}(M^{-1}\hat{\mathbf{x}}),\tilde{\mathbf{H}}(M^{-1}\hat{\mathbf{x}}))$ satisfy the transformed isotropic Maxwell's equations:

$$\begin{cases} \nabla\times\hat{\mathbf{E}} - i\omega\mu_r\hat{\mathbf{H}} = \mathbf{0}, \\ \nabla\times\hat{\mathbf{H}} + i\omega\varepsilon_r\hat{\mathbf{E}} = \mathbf{0}, \\ \nabla\cdot(\varepsilon_r\hat{\mathbf{E}}) = 0, \\ \nabla\cdot(\mu_r\hat{\mathbf{H}}) = 0, \end{cases} \quad \text{in } \hat{\Omega}, \tag{2.10}$$

with the original absorbing boundary condition

$$\mathbf{H}\times\mathbf{n} - \vartheta(\mathbf{n}\times\mathbf{E})\times\mathbf{n} = \mathbf{g}/i\omega \quad \text{on} \quad \hat{\gamma} = \partial\hat{\Omega}. \tag{2.11}$$

Here, $\mathbf{n}$ and $\hat{\mathbf{n}}$ are the unit out normal vectors of the boundary $\partial\Omega$ and $\partial\hat{\Omega}$, respectively. Moreover, we have $\mathbf{n} = M^T\hat{\mathbf{n}}/|M^T\hat{\mathbf{n}}|$.

Finally, the physical electromagnetic fields $\big(\mathbf{E}(\mathbf{x}),\mathbf{H}(\mathbf{x})\big)$ satisfying

$$\begin{aligned} \mathbf{E}(\mathbf{x}) &= G\tilde{\mathbf{E}}(\mathbf{x}) = G\tilde{\mathbf{E}}(M^{-1}\hat{\mathbf{x}}) = G\hat{\mathbf{E}}(\hat{\mathbf{x}}), \\ \mathbf{H}(\mathbf{x}) &= \frac{1}{i\omega}\mu^{-1}\nabla\times\mathbf{E}(\mathbf{x}) \end{aligned} \tag{2.12}$$

is the solution of the original anisotropic Maxwell equations (2.2).

3 The PWDG method

We derive the PWDG method introduced in [8] from the original anisotropic Maxwell equations (2.2)-(2.3) satisfied by the physical electromagnetic fields (**E**,**H**).

Define the Trefftz spaces as follows:

$$\mathbf{V}^E(\Omega_k)=\Big\{\mathbf{F}\in H(\mathrm{curl},\Omega_k);\ \nabla\times\Big(\frac{1}{i\omega}\mu^{-1}\nabla\times\mathbf{F}\Big)+i\omega\varepsilon\mathbf{F}=\mathbf{0}\Big\}, \tag{3.1}$$

$$\mathbf{V}^H(\Omega_k)=\Big\{\mathbf{G}\in H(\mathrm{curl},\Omega_k);\ \mathbf{G}=\nabla\times\mathbf{F},\ \text{where}\ \ \mathbf{F}\in\mathbf{V}^E(\Omega_k)\Big\}$$

and

$$\mathbf{V}(\mathcal{T}_h)=\Big\{\mathbf{F}\in(L^2(\Omega))^3;\ \mathbf{F}\in\mathbf{V}^E(\Omega_k)\ \text{on each}\ \ \Omega_k\Big\}.$$

In order to derive the PWDG method, set

$$\mathbf{V}(\Omega_k)=\big\{\mathbf{v}\in H(\mathrm{curl},\Omega_k),\ \mathbf{n}\times\mathbf{v}\in L^2_{\mathbf{T}}(\partial\Omega_k)\big\}. \tag{3.2}$$

Integrating by parts the Eq. (2.2) for every $\Omega_k\in\mathcal{T}_h$, we get the equations of the vector-valued functions $(\mathbf{E},\mathbf{H})\in\mathbf{V}(\Omega_k)\times\mathbf{V}(\Omega_k)$

$$\begin{cases} i\omega\displaystyle\int_{\Omega_k}\mathbf{H}\cdot\overline{\boldsymbol{\psi}}d\mathbf{x}-\int_{\Omega_k}\mathbf{E}\cdot\overline{\nabla\times(\mu^{-1}\boldsymbol{\psi})}d\mathbf{x}-\int_{\partial\Omega_k}\mathbf{n}\times\mathbf{E}\cdot\overline{(\mu^{-1}\boldsymbol{\psi})}dS=0, & \forall\boldsymbol{\psi}\in\mathbf{V}(\Omega_k),\\ i\omega\displaystyle\int_{\Omega_k}\varepsilon\mathbf{E}\cdot\overline{\boldsymbol{\xi}}d\mathbf{x}+\int_{\Omega_k}\mathbf{H}\cdot\overline{\nabla\times\boldsymbol{\xi}}d\mathbf{x}+\int_{\partial\Omega_k}\mathbf{n}\times\mathbf{H}\cdot\overline{\boldsymbol{\xi}}dS=0, & \forall\boldsymbol{\xi}\in\mathbf{V}(\Omega_k). \end{cases} \tag{3.3}$$

Then the above problem can be discretized as follows: for every $\Omega_k\in\mathcal{T}_h$, the vector-valued functions $(\mathbf{E}_h,\mathbf{H}_h)\in\mathbf{V}_p^E(\Omega_k)\times\mathbf{V}_p^H(\Omega_k)$ satisfy

$$\begin{cases} i\omega\displaystyle\int_{\Omega_k}\mathbf{H}_h\cdot\overline{\boldsymbol{\psi}_{h,p}}\,d\mathbf{x}-\int_{\Omega_k}\mathbf{E}_h\cdot\overline{\nabla\times(\mu^{-1}\boldsymbol{\psi}_{h,p})}\,d\mathbf{x}-\int_{\partial\Omega_k}\mathbf{n}\times\widehat{\mathbf{E}}_h\cdot\overline{(\mu^{-1}\boldsymbol{\psi}_{h,p})}\,dS=0,\\ \qquad\qquad\qquad\qquad\qquad\qquad\qquad\qquad\forall\boldsymbol{\psi}_{h,p}\in\mathbf{V}_p^H(\Omega_k),\\ i\omega\displaystyle\int_{\Omega_k}\varepsilon\mathbf{E}_h\cdot\overline{\boldsymbol{\xi}_{h,p}}\,d\mathbf{x}+\int_{\Omega_k}\mathbf{H}_h\cdot\overline{\nabla\times\boldsymbol{\xi}_{h,p}}\,d\mathbf{x}+\int_{\partial\Omega_k}\mathbf{n}\times\widehat{\mathbf{H}}_h\cdot\overline{\boldsymbol{\xi}_{h,p}}\,dS=0,\\ \qquad\qquad\qquad\qquad\qquad\qquad\qquad\qquad\forall\boldsymbol{\xi}_{h,p}\in\mathbf{V}_p^E(\Omega_k), \end{cases} \tag{3.4}$$

where $\mathbf{V}_p^E(\Omega_k)\subset\mathbf{V}^E(\Omega_k)\subset\mathbf{V}(\Omega_k)$ and $\mathbf{V}_p^H(\Omega_k)\subset\mathbf{V}^H(\Omega_k)\subset\mathbf{V}(\Omega_k)$ are discretized spaces, and $\widehat{\mathbf{E}}_h$ and $\widehat{\mathbf{H}}_h$ on $\mathcal{F}_h$ are the single-valued numerical fluxes to be specified.

By the assumption $\nabla\times\mathbf{V}_p^E(\Omega_k)\subset\mathbf{V}_p^H(\Omega_k)$, we select $\boldsymbol{\psi}_{h,p}=\nabla\times\boldsymbol{\xi}_{h,p}$ in the first equation of (3.4) and get

$$i\omega\int_{\Omega_k}\mathbf{H}_h\cdot\overline{\nabla\times\boldsymbol{\xi}_{h,p}}\,d\mathbf{x}=\int_{\Omega_k}\mathbf{E}_h\cdot\overline{\nabla\times(\mu^{-1}\nabla\times\boldsymbol{\xi}_{h,p})}\,d\mathbf{x}+\int_{\partial\Omega_k}\mathbf{n}\times\widehat{\mathbf{E}}_h\cdot\overline{(\mu^{-1}\nabla\times\boldsymbol{\xi}_{h,p})}\,dS.$$

Substituting this equation into the second equation of (3.4) leads to

$$\int_{\Omega_k} \mathbf{E}_h \cdot \overline{\nabla\times(\mu^{-1}\nabla\times\boldsymbol{\xi}_{h,p})-\omega^2\varepsilon\boldsymbol{\xi}_{h,p}}\, d\mathbf{x} + \int_{\partial\Omega_k} \mathbf{n}\times\widehat{\mathbf{E}}_h\cdot\overline{(\mu^{-1}\nabla\times\boldsymbol{\xi}_{h,p})}\, dS$$
$$+i\omega\int_{\partial\Omega_k}\mathbf{n}\times\widehat{\mathbf{H}}_h\cdot\overline{\boldsymbol{\xi}_{h,p}}\, dS=0, \quad \forall\boldsymbol{\xi}_{h,p}\in\mathbf{V}_p^E(\Omega_k).$$

Using the Trefftz property (3.1) satisfied by the test function $\boldsymbol{\xi}_{h,p}$, we can obtain the elemental equation defining the PWDG method

$$\int_{\partial\Omega_k} \mathbf{n}\times\widehat{\mathbf{E}}_h\cdot\overline{(\mu^{-1}\nabla\times\boldsymbol{\xi}_{h,p})}\, dS + i\omega\int_{\partial\Omega_k}\mathbf{n}\times\widehat{\mathbf{H}}_h\cdot\overline{\boldsymbol{\xi}_{h,p}}\, dS=0, \quad \forall\boldsymbol{\xi}_{h,p}\in\mathbf{V}_p^E(\Omega_k). \tag{3.5}$$

In analogy to the isotropic Maxwell's case considered in [8], we define the numerical fluxes on $\mathcal{F}_h^{\mathrm{I}}$:

$$\begin{cases} \widehat{\mathbf{E}}_h=\{\{\mathbf{E}_h\}\}-\dfrac{\beta}{i\omega}[\![\mu^{-1}\nabla_h\times\mathbf{E}_h]\!]_T, \\ \widehat{\mathbf{H}}_h=\dfrac{1}{i\omega}\{\{\mu^{-1}\nabla_h\times\mathbf{E}_h\}\}+\alpha[\![\mathbf{E}_h]\!]_T, \end{cases} \tag{3.6}$$

and on $\mathcal{F}_h^{\mathrm{B}}$:

$$\begin{cases} \widehat{\mathbf{E}}_h=\mathbf{E}_h-\delta\vartheta^{-1}\left(\dfrac{1}{i\omega}\mathbf{n}\times(\mu^{-1}\nabla_h\times\mathbf{E}_h)+\vartheta(\mathbf{n}\times\mathbf{E}_h)\times\mathbf{n}+\dfrac{1}{i\omega}\mathbf{g}\right), \\ \widehat{\mathbf{H}}_h=\dfrac{1}{i\omega}\mu^{-1}\nabla_h\times\mathbf{E}_h-(1-\delta)\left(\dfrac{1}{i\omega}\mu^{-1}\nabla_h\times\mathbf{E}_h-\vartheta(\mathbf{n}\times\mathbf{E}_h)-\dfrac{1}{i\omega}\mathbf{n}\times\mathbf{g}\right), \end{cases} \tag{3.7}$$

where ∇_h denotes the element application of the ∇ operator, α,β,δ are strictly positive constants, with $0<\delta\le 1/2$.

Defining the finite dimensional discretized space

$$\mathbf{V}_p(\mathcal{T}_h)=\left\{\mathbf{F}_h\in(L^2(\Omega))^3;\ \mathbf{F}_h\in\mathbf{V}_p^E(\Omega_k) \text{ on each } \Omega_k\right\},$$

inserting the numerical fluxes into (3.5) and adding over all elements finish the definition of the PWDG method: find $\mathbf{E}_h\in\mathbf{V}_p(\mathcal{T}_h)$ such that,

$$\mathcal{A}_h(\mathbf{E}_h,\boldsymbol{\xi}_{h,p})=\ell_h(\boldsymbol{\xi}_{h,p}), \quad \forall\boldsymbol{\xi}_{h,p}\in\mathbf{V}_p(\mathcal{T}_h), \tag{3.8}$$

where

$$\mathcal{A}_h(\mathbf{E},\boldsymbol{\xi})=-\int_{\mathcal{F}_h^{\mathrm{I}}}\{\{\mathbf{E}\}\}\cdot\overline{[\![\mu^{-1}\nabla_h\times\boldsymbol{\xi}]\!]_T}\, dS-i\omega^{-1}\int_{\mathcal{F}_h^{\mathrm{I}}}\beta[\![\mu^{-1}\nabla_h\times\mathbf{E}]\!]_T\cdot\overline{[\![\mu^{-1}\nabla_h\times\boldsymbol{\xi}]\!]_T}\, dS$$
$$-\int_{\mathcal{F}_h^{\mathrm{I}}}\{\{\mu^{-1}\nabla_h\times\mathbf{E}\}\}\cdot\overline{[\![\boldsymbol{\xi}]\!]_T}\, dS-i\omega\int_{\mathcal{F}_h^{\mathrm{I}}}\alpha[\![\mathbf{E}]\!]_T\cdot\overline{[\![\boldsymbol{\xi}]\!]_T}\, dS$$
$$+\int_{\mathcal{F}_h^{\mathrm{B}}}(1-\delta)(\mathbf{n}\times\mathbf{E})\cdot\overline{(\mu^{-1}\nabla_h\times\boldsymbol{\xi})}\, dS$$

$$-i\omega^{-1}\int_{\mathcal{F}_h^{\rm B}}\delta\vartheta^{-1}[\mathbf{n}\times(\mu^{-1}\nabla_h\times\mathbf{E})]\cdot\overline{[\mathbf{n}\times(\mu^{-1}\nabla_h\times\boldsymbol{\xi})]}\,dS$$
$$-\int_{\mathcal{F}_h^{\rm B}}\delta(\mu^{-1}\nabla_h\times\mathbf{E})\cdot\overline{(\mathbf{n}\times\boldsymbol{\xi})}\,dS-i\omega\int_{\mathcal{F}_h^{\rm B}}(1-\delta)\vartheta(\mathbf{n}\times\mathbf{E})\cdot\overline{(\mathbf{n}\times\boldsymbol{\xi})}\,dS$$

and

$$\ell_h(\boldsymbol{\xi})=-i\omega^{-1}\int_{\mathcal{F}_h^{\rm B}}\delta\vartheta^{-1}(\mathbf{n}\times\mathbf{g})\cdot\overline{\mu^{-1}\nabla_h\times\boldsymbol{\xi}}\,dS+\int_{\mathcal{F}_h^{\rm B}}(1-\delta)(\mathbf{n}\times\mathbf{g})\cdot\overline{(\mathbf{n}\times\boldsymbol{\xi})}\,dS. \tag{3.9}$$

Remark 3.1. We have derived the PWDG method from the original anisotropic Maxwell equations (2.2) satisfied by the physical electromagnetic field (**E**,**H**). Of course, we can also derive another variational formulation from the transformed isotropic Maxwell equations (2.10)-(2.11) satisfied by the scaled electric and magnetic fields ($\hat{\mathbf{E}}$,$\hat{\mathbf{H}}$). For this way, the transformed computational domain $\hat{\Omega}$ should be computed before deriving the variational formulation of the transformed isotropic Maxwell equations. After obtaining the approximations defined on the triangulation $\hat{\mathcal{T}}_{\hat{h}}$ generated by the variational formulation, the numerical solutions of the original problem (2.3) defined on the triangulation $\mathcal{T}_h$ can be computed by the transformations. However, there are some drawbacks for this way:

(i) If the computational domain Ω is complicated, implementing the transformation is not a simple job.

(ii) Due to the appearance of the original boundary condition (2.3), the computation of the involved boundary integral defined on $\hat{\mathcal{F}}_{\hat{h}}^{\rm B}$ is more difficult than that defined on $\mathcal{F}_h^{\rm B}$.

Remark 3.2. The variational formulation of the PWDG method introduced in this section would remain unchanged if the material coefficients were constant on the whole domain, namely, the media are isotropic. Thus, the proposed method can be viewed as an extension of the existing method introduced in [8] to the case of anisotropic media.

4 Discretization of the variational problems

The discretization is based on a finite-dimensional space $\mathbf{V}_p(\mathcal{T}_h)\subset\mathbf{V}(\mathcal{T}_h)$. In this subsection, we first give the precise definition of such a space $\mathbf{V}_p(\mathcal{T}_h)$.

In practice, by choosing p unit propagation directions $\mathbf{d}_l$, $l=1,\cdots,p$ (we use the optimal spherical codes from [26]), we can define the plane wave functions $\hat{\mathbf{E}}_l$:

$$\hat{\mathbf{E}}_l=\mathbf{F}_l\exp(\mathrm{i}\,\kappa\,\mathbf{d}_l\cdot\hat{\mathbf{x}})\quad\text{and}\quad\hat{\mathbf{E}}_{l+p}=\mathbf{G}_l\exp(\mathrm{i}\,\kappa\,\mathbf{d}_l\cdot\hat{\mathbf{x}})\quad(l=1,\cdots,p), \tag{4.1}$$

where $\kappa=\omega\sqrt{\mu_r\varepsilon_r}$, $\mathbf{F}_l$ and $\mathbf{G}_l$ are polarization vectors, satisfying $\mathbf{F}_l\cdot\mathbf{d}_l=0$ and $\mathbf{G}_l=\mathbf{F}_l\times\mathbf{d}_l$ $(l=1,\cdots,p)$. Let the number p of plane wave propagation directions be chosen as $p=(m+1)^2$ in 3D.

Let $\hat{\mathcal{Q}}_{2p}$ denote the space spanned by the $2p$ plane wave functions $\hat{\mathbf{E}}_l$ $(l=1,\cdots,2p)$. Define the transformed plane wave space

$$\hat{\mathbf{V}}_p(\hat{\mathcal{T}}_h)=\big\{\mathbf{v}\in L^2(\hat{\Omega}):\ \mathbf{v}|_{\hat{K}}\in\hat{\mathcal{Q}}_{2p}\ \text{ for any }\ \hat{K}\in\hat{\mathcal{T}}_h\big\}. \tag{4.2}$$

It can be seen that $\hat{\mathbf{E}}_l$ $(l=1,\cdots,2p)$ satisfies the transformed isotropic Maxwell equations (2.10). By (2.12), we can define the anisotropic plane wave basis functions satisfying the original equations (2.2):

$$\mathbf{E}_l=G\,\mathbf{F}_l\exp(\mathrm{i}\,\kappa\,\mathbf{d}_l\cdot M\mathbf{x})\quad\text{and}\quad\mathbf{E}_{l+p}=G\,\mathbf{G}_l\exp(\mathrm{i}\,\kappa\,\mathbf{d}_l\cdot M\mathbf{x})\quad(l=1,\cdots,p). \tag{4.3}$$

Let $\mathcal{Q}_{2p}$ denote the space spanned by the $2p$ plane wave functions $\mathbf{E}_l$ $(l=1,\cdots,2p)$. Define the plane wave space

$$\mathbf{V}_p(\mathcal{T}_h)=\big\{\mathbf{v}\in L^2(\Omega):\ \mathbf{v}|_K\in\mathcal{Q}_{2p}\ \text{ for any }\ K\in\mathcal{T}_h\big\}. \tag{4.4}$$

It is clear that the above space has $N\times 2p$ basis functions, which are defined by

$$\boldsymbol{\phi}_l^k(\mathbf{x})=\begin{cases}\mathbf{E}_l(\mathbf{x}), & \mathbf{x}\in\Omega_k,\\ 0, & \mathbf{x}\in\Omega_j\ \text{ satisfying }\ j\neq k,\end{cases}\qquad(k=1,\cdots,N;\quad l=1,\cdots,2p). \tag{4.5}$$

5 Error estimates of the approximate solutions in anisotropic media

For a bounded and connected domain $D\subset\Omega$, let $||\cdot||_{s,\omega,D}$ be the ω-weighted Sobolev norm defined by

$$||v||^2_{s,\omega,D}=\sum_{j=0}^{s}\omega^{2(s-j)}|v|^2_{j,D}.$$

In the rest of the paper, we denote $||M||_2$ by $||M||$ for the given matrix M, and the condition number $\text{cond}(\Lambda)$ by ρ for the diagonal matrix Λ defined in (1.1).

Let the mesh triangulation $\mathcal{T}_h$ satisfy the definition stated in [8, Sec 5], and set $\lambda=\min_{\Omega_k\in\mathcal{T}_h}\lambda_k$, where λ_k is the positive parameter depending only on the shape of an element Ω_k of $\mathcal{T}_h$ introduced in [20, Th. 3.2]. Under the coordinate transformation (2.9), set $\hat{\lambda}=\min_{\hat{\Omega}_k\in\hat{\mathcal{T}}_{\hat{h}}}\hat{\lambda}_k$. Let r and m be given positive integers satisfying $m\geq 2r+1$ and $m\geq 2(1+2^{1/\hat{\lambda}})$.

Lemma 5.3 and Lemma 5.5 state the transformation stability with respect to a mesh-dependent norm and a mesh-independent norm, respectively, which are first proved and commented. To our knowledge, there are no similar stability estimates for the plane wave methods in the existing literature. Then by the known approximate result in Lemma 5.4, we can prove the desired error estimates (see Theorem 5.1).

5.1 Error estimates in mesh-skeleton norm

Define the broken Sobolev space

$$H^r(\text{curl};\mathcal{T}_h)=\{\mathbf{w}\in L^2(\Omega)^3:\mathbf{w}|_{\Omega_k}\in H^r(\text{curl};\Omega_k),\quad \forall\Omega_k\in\mathcal{T}_h\}. \tag{5.1}$$

Let $\mathbf{T}(\mathcal{T}_h)$ be the piecewise Trefftz space defined on $\mathcal{T}_h$ by

$$\begin{aligned}\mathbf{T}(\mathcal{T}_h)=\Big\{&\mathbf{w}\in L^2(\Omega)^3:\exists s>0\ s.t.\ \mathbf{w}\in H^{1/2+s}(\text{curl};\mathcal{T}_h),\\ &\text{and}\quad \nabla\times(\mu^{-1}\nabla\times\mathbf{w})-\omega^2\varepsilon\mathbf{w}=\mathbf{0}\quad\text{in each}\quad \Omega_k\in\mathcal{T}_h\Big\}.\end{aligned} \tag{5.2}$$

We endow $\mathbf{T}(\mathcal{T}_h)$ with the mesh-skeleton norm

$$\begin{aligned}|||\mathbf{w}|||^2_{\mathcal{F}_h}=&\omega^{-1}||\beta^{1/2}[\![\mu^{-1}\nabla_h\times\mathbf{w}]\!]_T||^2_{0,\mathcal{F}_h^I}+\omega||\alpha^{1/2}[\![\mathbf{w}]\!]_T||^2_{0,\mathcal{F}_h^I}\\ &+\omega^{-1}||\delta^{1/2}\vartheta^{-1/2}\mathbf{n}\times(\mu^{-1}\nabla_h\times\mathbf{w})||^2_{0,\mathcal{F}_h^B}+\omega||(1-\delta)^{1/2}\vartheta^{1/2}\mathbf{n}\times\mathbf{w}||^2_{0,\mathcal{F}_h^B}\end{aligned} \tag{5.3}$$

and the following augmented norm on $\mathbf{T}(\mathcal{T}_h)$:

$$\begin{aligned}|||\mathbf{w}|||^2_{\mathcal{F}_h^+}=&|||\mathbf{w}|||^2_{\mathcal{F}_h}+\omega||\beta^{-1/2}\{\{\mathbf{w}\}\}||^2_{0,\mathcal{F}_h^I}+\omega^{-1}||\alpha^{-1/2}\{\{\mu^{-1}\nabla_h\times\mathbf{w}\}\}||^2_{0,\mathcal{F}_h^I}\\ &+\omega||\delta^{-1/2}\vartheta^{1/2}(\mathbf{n}\times\mathbf{w})||^2_{0,\mathcal{F}_h^B}.\end{aligned} \tag{5.4}$$

Before deriving the desired estimates, we recall the following existence, uniqueness and continuity results of solutions to the PWDG method (see [8]).

Lemma 5.1. *There exists a unique* $\mathbf{E}_h$ *solution to* (3.8) *moreover, we have*

$$\begin{aligned}&-Im[\mathcal{A}_h(\mathbf{w},\mathbf{w})]=|||\mathbf{w}|||^2_{\mathcal{F}_h},\\ &|\mathcal{A}_h(\mathbf{w},\boldsymbol{\xi})|\le 2|||\mathbf{w}|||_{\mathcal{F}_h^+}\,|||\boldsymbol{\xi}|||_{\mathcal{F}_h},\quad \forall\ \mathbf{w},\boldsymbol{\xi}\in\mathbf{T}(\mathcal{T}_h).\end{aligned} \tag{5.5}$$

The following abstract error estimate (see [8]) in the $|||\cdot|||_{\mathcal{F}_h}-$norm also holds in the current situation.

Lemma 5.2. *Assume that the analytical solution* $\mathbf{E}$ *to the Maxwell equations* (2.2) *in anisotropic media belongs to* $\mathbf{T}(\mathcal{T}_h)$. *Then we have*

$$|||\mathbf{E}-\mathbf{E}_h|||_{\mathcal{F}_h}\le 3\inf_{\boldsymbol{\xi}_{h,p}\in\mathbf{V}_p(\mathcal{T}_h)}|||\mathbf{E}-\boldsymbol{\xi}_h|||_{\mathcal{F}_h^+}. \tag{5.6}$$

By the transformation (2.12), we can obtain the following main lemma.

Lemma 5.3. *Assume that the analytical solution* $\mathbf{E}$ *to the Maxwell equations* (2.2) *in anisotropic media belongs to* $\mathbf{T}(\mathcal{T}_h)$. *Then we obtain*

$$|||\mathbf{E}|||_{\mathcal{F}_h} \leq C\,\rho\,|||\hat{\mathbf{E}}|||_{\hat{\mathcal{F}}_{\hat{h}}} \tag{5.7}$$

and

$$|||\mathbf{E}|||_{\mathcal{F}_h^+} \leq C\,\rho\,|||\hat{\mathbf{E}}|||_{\hat{\mathcal{F}}_{\hat{h}}^+}, \tag{5.8}$$

where ρ *is the condition number of the matrix* Λ. *The constant* C *depends on* $||M^{-1}||$, *and* $|||\hat{\mathbf{E}}|||_{\hat{\mathcal{F}}_{\hat{h}}}$ *and* $|||\hat{\mathbf{E}}|||_{\hat{\mathcal{F}}_{\hat{h}}^+}$ *are defined by* (5.3) *and* (5.4) *respectively, where* μ *is replaced by* μ_r.

Proof. We divide the proof into three steps.

Step 1: The estimates of $\big|\big|[\![\mu^{-1}\nabla_h\times\mathbf{E}]\!]_T\big|\big|_{0,\mathcal{F}_h^I}$ and $\big|\big|\mathbf{n}\times(\mu^{-1}\nabla_h\times\mathbf{E})\big|\big|_{0,\mathcal{F}_h^B}$.

By the scaling transformation (2.4) and the direct calculation, we obtain

$$\nabla\times\mathbf{E}=\nabla\times(G\,\tilde{\mathbf{E}})=\sqrt{a_x}\,\Lambda^{1/2}\,\nabla_{\mathbf{a}}\times\tilde{\mathbf{E}}. \tag{5.9}$$

Then we can show that

$$\mu^{-1}\nabla\times\mathbf{E}=\sqrt{a_x}\,\mu_r^{-1}\,\Lambda^{-1/2}\nabla_{\mathbf{a}}\times\tilde{\mathbf{E}}. \tag{5.10}$$

Thus, on the interface $\Gamma_{kj}\in\mathcal{F}_h^I$ we have

$$[\![\mu^{-1}\nabla_h\times\mathbf{E}]\!]_T=\sqrt{a_x}\,\mu_r^{-1}\,\big(\mathbf{n}_k\times(\Lambda^{-1/2}\nabla_{\mathbf{a}}\times\tilde{\mathbf{E}}_k)+\mathbf{n}_j\times(\Lambda^{-1/2}\nabla_{\mathbf{a}}\times\tilde{\mathbf{E}}_j)\big). \tag{5.11}$$

By the coordinate transformation (2.9), we know that

$$\left(\frac{|\Gamma_{kj}|}{|\hat{\Gamma}_{kj}|}\right)^{1/2}\leq||M^{-1}||,\quad \mathbf{n}_k=|M^{-T}\mathbf{n}|\,M^T\hat{\mathbf{n}}_k \tag{5.12}$$

and

$$\nabla_{\mathbf{a}}\times\tilde{\mathbf{E}}_k=\nabla_{\hat{h}}\times\hat{\mathbf{E}}_k. \tag{5.13}$$

Thus we have

$$\begin{aligned}\mathbf{n}_k\times(\Lambda^{-1/2}\nabla_{\mathbf{a}}\times\tilde{\mathbf{E}}_k)&=|M^{-T}\mathbf{n}|\,(M^T\hat{\mathbf{n}}_k)\times(\Lambda^{-1/2}\nabla_{\hat{h}}\times\hat{\mathbf{E}}_k)\\&=|M^{-T}\mathbf{n}|\,\Lambda^{1/2}\hat{\mathbf{n}}_k\times(\nabla_{\hat{h}}\times\hat{\mathbf{E}}_k).\end{aligned} \tag{5.14}$$

Then by (5.11) and (5.14), we can deduce that

$$[\![\mu^{-1}\nabla_h\times\mathbf{E}]\!]_T=\sqrt{a_x}\,|M^{-T}\mathbf{n}|\Lambda^{1/2}[\![\mu_r^{-1}(\nabla_{\hat{h}}\times\hat{\mathbf{E}})]\!]_T. \tag{5.15}$$

Combing (5.12) and (5.15) with

$$\sqrt{a_x}\,||M^{-T}||\,||\Lambda^{1/2}||\leq\rho$$

yields

$$||[\![\mu^{-1}\nabla_h\times\mathbf{E}]\!]_T||_{0,\mathcal{F}_h^I}\leq\sqrt{a_x}\,||M^{-T}||\,||\Lambda^{1/2}||\,||M^{-1}||\,||[\![\mu_r^{-1}\nabla_{\hat{h}}\times\hat{\mathbf{E}}]\!]_T||_{0,\hat{\mathcal{F}}_h^I}$$
$$\leq\rho\,||M^{-1}||\,||[\![\mu_r^{-1}\nabla_{\hat{h}}\times\hat{\mathbf{E}}]\!]_T||_{0,\hat{\mathcal{F}}_{\hat{h}}^I} \tag{5.16}$$

and

$$||\mathbf{n}\times(\mu^{-1}\nabla_h\times\mathbf{E})||_{0,\mathcal{F}_h^B}\leq\rho\,||M^{-1}||\,||\hat{\mathbf{n}}\times(\mu_r^{-1}\nabla_{\hat{h}}\times\hat{\mathbf{E}})||_{0,\hat{\mathcal{F}}_{\hat{h}}^B}. \tag{5.17}$$

Step 2: The estimates of $||[\![\mathbf{E}]\!]_T||_{0,\mathcal{F}_h^I}$ and $||\mathbf{n}\times\mathbf{E}||_{0,\mathcal{F}_h^B}$.

By the scaling transformation (2.4) and (5.12), we obtain

$$\mathbf{n}_k\times\mathbf{E}_k=|M^{-T}\mathbf{n}_k|\;(M^T\hat{\mathbf{n}}_k)\times G\tilde{\mathbf{E}}_k. \tag{5.18}$$

Define the matrix $\tilde{M}=\mathrm{diag}(a_x,s_z,s_y)$. By the direct manipulation, we can show that

$$\mathbf{n}_k\times\mathbf{E}_k=|M^{-T}\mathbf{n}_k|\;\tilde{M}\hat{\mathbf{n}}_k\times\tilde{\mathbf{E}}_k=|M^{-T}\mathbf{n}_k|\;\tilde{M}\;\hat{\mathbf{n}}_k\times\hat{\mathbf{E}}_k. \tag{5.19}$$

Combing (5.19) with

$$||M^{-T}||\;||\tilde{M}||\leq\rho$$

yields

$$||[\![\mathbf{E}]\!]_T||_{0,\mathcal{F}_h^I}\leq\rho\,||M^{-1}||\,||[\![\hat{\mathbf{E}}]\!]_T||_{0,\hat{\mathcal{F}}_{\hat{h}}^I},$$
$$||\mathbf{n}\times\mathbf{E}||_{0,\mathcal{F}_h^B}\leq\rho\,||M^{-1}||\,||\hat{\mathbf{n}}\times\hat{\mathbf{E}}||_{0,\hat{\mathcal{F}}_{\hat{h}}^B}. \tag{5.20}$$

Step 3: The estimates of $||\{\{\mathbf{E}\}\}||_{0,\mathcal{F}_h^I}$, $||\{\{\mu^{-1}\nabla_h\times\mathbf{E}\}\}||_{0,\mathcal{F}_h^I}$ and $||(\mathbf{n}\times\mathbf{E})||_{0,\mathcal{F}_h^B}$.

By the scaling transformation (2.4) and the coordinate transformation (2.9), we get

$$||\{\{\mathbf{E}\}\}||_{0,\mathcal{F}_h^I}=||\{\{G\tilde{\mathbf{E}}\}\}||_{0,\mathcal{F}_h^I}\leq||G||_2\;||\{\{\tilde{\mathbf{E}}\}\}||_{0,\mathcal{F}_h^I}\leq\rho^{1/2}\;||M^{-1}||\;||\{\{\hat{\mathbf{E}}\}\}||_{0,\hat{\mathcal{F}}_h^I}. \tag{5.21}$$

Moreover, we have

$$\begin{aligned}||\{\{\mu^{-1}\nabla_h\times\mathbf{E}\}\}||_{0,\mathcal{F}_h^I}&=||\{\{\mu_r^{-1}\Lambda^{-1}\,(\nabla_h\times(G\tilde{\mathbf{E}}))\}\}||_{0,\mathcal{F}_h^I}\\&\overset{(5.10)}{=\!=}||\{\{\sqrt{a_x}\mu_r^{-1}\Lambda^{-1/2}\,(\nabla_{\mathbf{a}}\times\tilde{\mathbf{E}})\}\}||_{0,\mathcal{F}_h^I}\\&\overset{(5.13)}{=\!=}||\{\{\sqrt{a_x}\mu_r^{-1}\Lambda^{-1/2}\,(\nabla_{\hat{h}}\times\hat{\mathbf{E}})\}\}||_{0,\mathcal{F}_h^I}\\&\leq\rho^{1/2}\,||M^{-1}||\,||\{\{\mu_r^{-1}\nabla_{\hat{h}}\times\hat{\mathbf{E}}\}\}||_{0,\hat{\mathcal{F}}_{\hat{h}}^I},\end{aligned} \tag{5.22}$$

and

$$||(\mathbf{n}\times\mathbf{E})||_{0,\mathcal{F}_h^B}\overset{(5.20)}{\leq}\rho\,||M^{-1}||\,||(\hat{\mathbf{n}}\times\hat{\mathbf{E}})||_{0,\hat{\mathcal{F}}_{\hat{h}}^B}. \tag{5.23}$$

Combing (5.16)-(5.17) with (5.20)-(5.23) yields the desired result (5.8). □

The following approximate result thanks to Corollary 5.5 in [8] (for ease of notation, we only give a simplified form of the result).

Lemma 5.4. *Assume that the analytical solution* $\hat{\mathbf{E}}\in H^{r+1}(curl;\hat{\mathcal{T}}_{\hat{h}})$ *satisfies the Maxwell equations* (2.10) *in isotropic media. Choosing a set of* $p=(m+1)^2$ *plane wave propagation directions* $\{\mathbf{d}_l\}_{1\leq l\leq p}$ *with the corresponding set of polarization directions* $\mathbf{F}_l,\mathbf{G}_l$ *defined by* (4.1) *in a suitable manner, where* $m,r\in\mathbf{N}$ *and* $m\geq 2r+1$. *Then, there exists* $\hat{\boldsymbol{\xi}}_{\hat{h}}\in\hat{\mathbf{V}}_p(\hat{\mathcal{T}}_{\hat{h}})$ *such that*

$$|||\hat{\mathbf{E}}-\hat{\boldsymbol{\xi}}_{\hat{h}}|||_{\hat{\mathcal{F}}^+_{\hat{h}}}\leq C\omega^{-5/2}\left(\frac{\hat{h}}{m^{\hat{\lambda}}}\right)^{r-3/2}||\nabla_{\hat{h}}\times\hat{\mathbf{E}}||_{r+1,\omega,\hat{\Omega}}, \tag{5.24}$$

where $C=C(\omega h)>0$ *is independent of* p *and* $\hat{\mathbf{E}}$, *but increases as a function of the product* ωh, *and* C *depends on the shape of the* $\hat{\Omega}_k\in\hat{\mathcal{T}}_h,r,\vartheta,\varepsilon_r,\mu_r$ *and on the flux parameters.*

5.2 Transformation stability with respect to a mesh-independent norm

We introduce the following slightly modified weaker norms (refer to [8]): for every $\mathbf{w}\in L^2(\Omega)^3$ and $\hat{\mathbf{w}}\in L^2(\hat{\Omega})^3$,

$$||\mathbf{w}||_{\tilde{H}(\div;\Omega)'}:=\sup_{\mathbf{v}\in\tilde{H}(\div;\Omega)}\left(\left(\int_\Omega G^{-1}\mathbf{w}\cdot\mathbf{v}\,d\mathbf{x}\right)/||\mathbf{v}||_{\tilde{H}(\div;\Omega)}\right) \tag{5.25}$$

and

$$||\hat{\mathbf{w}}||_{H(\div;\hat{\Omega})'}:=\sup_{\hat{\mathbf{v}}\in H(\div;\hat{\Omega})}\left(\left(\int_{\hat{\Omega}}\hat{\mathbf{w}}\cdot\hat{\mathbf{v}}\,d\hat{\mathbf{x}}\right)/||\hat{\mathbf{v}}||_{H(\div;\hat{\Omega})}\right), \tag{5.26}$$

where $||\mathbf{v}||^2_{\tilde{H}(\div;\Omega)}=||\mathbf{v}||^2_{0,\Omega}+||\nabla_{\mathbf{a}}\cdot\mathbf{v}||^2_{0,\Omega}$ and $||\hat{\mathbf{v}}||^2_{H(\div;\hat{\Omega})}=||\hat{\mathbf{v}}||^2_{0,\hat{\Omega}}+||\nabla_{\hat{h}}\cdot\hat{\mathbf{v}}||^2_{0,\hat{\Omega}}$.

By the scaling transformation (2.4) and the coordinate transformation (2.9), we obtain the following lemma.

Lemma 5.5. *Assume that the analytical solution* $\mathbf{E}$ *to the Maxwell equations* (2.2) *in anisotropic media belongs to* $\mathbf{T}(\mathcal{T}_h)$. *Then*

$$||\mathbf{E}||_{\tilde{H}(\div;\Omega)'}\leq ||M^{-1}||^{3/2}\,||\hat{\mathbf{E}}||_{H(\div;\hat{\Omega})'}. \tag{5.27}$$

Proof. Let $\mathbf{E}\in\mathbf{T}(\mathcal{T}_h)$. Then

$$\begin{aligned}||\mathbf{E}||_{\tilde{H}(\div;\Omega)'}&\overset{(5.26)}{=\!=}\sup_{\mathbf{v}\in\tilde{H}(\div;\Omega)}\left(\left(\int_\Omega\tilde{\mathbf{E}}\cdot\mathbf{v}\,d\mathbf{x}\right)/||\mathbf{v}||_{\tilde{H}(\div;\Omega)}\right)\\&\overset{(2.9)}{=\!=}\sup_{\hat{\mathbf{v}}\in H(\div;\hat{\Omega})}\det(M^{-1/2})\left(\left(\int_{\hat{\Omega}}\hat{\mathbf{E}}\cdot\hat{\mathbf{v}}\,d\hat{\mathbf{x}}\right)/||\hat{\mathbf{v}}||_{H(\div;\hat{\Omega})}\right).\end{aligned} \tag{5.28}$$

This completes the proof. □

5.3 Error estimates

With the help of the above preparation, we can prove the final results easily.

Theorem 5.1. *Assume that the analytical solution* $\mathbf{E}\in H^{r+1}(curl;\Omega)$ $(r\in\mathbf{N})$ *satisfies the Maxwell equations* (2.2)-(2.3) *in anisotropic media. Let* $\mathbf{E}_h\in\mathbf{V}_p(\mathcal{T}_h)$ *(with* $p=(m+1)^2$*) be the solution of the discrete variational problem* (3.8)*, where* $m\in\mathbf{N}$ *and* $m\geq 2r+1$*. Then there exists a constant* C *independent of* p *but depending on* ω *and* h *through the product* ωh *as an increasing function, such that, for large* p,

$$|||\mathbf{E}-\mathbf{E}_h|||_{\mathcal{F}_h}\leq C\,\rho^{r/2+1}\,\omega^{-5/2}\left(\frac{h}{m^{\theta\lambda}}\right)^{r-3/2}||\nabla\times\mathbf{E}||_{r+1,\omega,\Omega'} \tag{5.29}$$

$$||\mathbf{E}-\mathbf{E}_h||_{\tilde{H}(\div;\Omega)'}\leq C\,\rho^{r/2-1/4}\,(\omega^{-5/2}+\omega^{-4})\frac{h^{r-2}}{m^{\theta\lambda(r-3/2)}}||\nabla\times\mathbf{E}||_{r+1,\omega,\Omega'} \tag{5.30}$$

where $C=C(\omega h)>0$ *depends on the shape of the* $\Omega_k\in\mathcal{T}_h,r,\vartheta,\varepsilon,\mu$ *and on the flux parameters, and* $\theta>0$ *depends on the coordinate transformation matrix* M.

Proof. With the transformations (2.4) and (2.9), we define $\boldsymbol{\xi}_h(\mathbf{x})=\mathbf{G}\,\hat{\boldsymbol{\xi}}_{\hat{\mathbf{h}}}(\mathbf{Mx})$, where $\hat{\boldsymbol{\xi}}_{\hat{h}}$ satisfying (5.24) denotes the plane wave approximation of the scaled electric field $\hat{\mathbf{E}}$. This, together with (5.6) and (5.8), leads to

$$\begin{aligned}|||\mathbf{E}-\mathbf{E}_h|||_{\mathcal{F}_h}&\leq C\,|||\mathbf{E}-\boldsymbol{\xi}_h|||_{\mathcal{F}_h^+}\leq C\,\rho\,|||\hat{\mathbf{E}}-\hat{\boldsymbol{\xi}}_{\hat{h}}|||_{\hat{\mathcal{F}}_{\hat{h}}^+}\\&\leq C\,\rho\,\omega^{-5/2}\left(\frac{\hat{h}}{m^{\hat{\lambda}}}\right)^{r-3/2}||\nabla_{\hat{h}}\times\hat{\mathbf{E}}||_{r+1,\omega,\hat{\Omega}}.\end{aligned}$$

By the transformation (2.12) and the direct calculation, yields

$$\big(\nabla_{\hat{h}}\times\hat{\mathbf{E}}\big)(\hat{\mathbf{x}})=\tilde{M}^{-1}\big(\nabla_h\times\mathbf{E}\big)(\mathbf{x}). \tag{5.31}$$

Then

$$\begin{aligned}|||\mathbf{E}-\mathbf{E}_h|||_{\mathcal{F}_h}&\leq C\,\rho\,\omega^{-5/2}\left(\frac{\hat{h}}{m^{\hat{\lambda}}}\right)^{r-3/2}||\tilde{M}^{-1}\nabla_h\times\mathbf{E}||_{r+1,\omega,\hat{\Omega}}\\&\leq C\,\rho\,\omega^{-5/2}\left(\frac{h}{m^{\theta\lambda}}\right)^{r-3/2}||M||^r||M^{-1}||^{r+2}||\nabla_h\times\mathbf{E}||_{r+1,\omega,\Omega}\\&\leq C\,\rho^{r/2+1}\,\omega^{-5/2}\left(\frac{h}{m^{\theta\lambda}}\right)^{r-3/2}||\nabla_h\times\mathbf{E}||_{r+1,\omega,\Omega}.\end{aligned} \tag{5.32}$$

To derive the second bound (5.30), we combine (5.27) with Lemma 5.5 and Proposition 4.8 given in [8], and we obtain

$$\begin{aligned}||\mathbf{E}-\mathbf{E}_h||_{\tilde{H}(\div;\Omega)'} &\leq C(\omega^{-5/2}+\omega^{-4})\frac{\hat{h}^{r-2}}{m^{\hat{\lambda}(r-3/2)}}\,||M^{-1}||^{3/2}\,||\nabla_{\hat{h}}\times\hat{\mathbf{E}}||_{r+1,\omega,\hat{\Omega}}\\ &\leq C(\omega^{-5/2}+\omega^{-4})\frac{h^{r-2}}{m^{\theta\lambda(r-3/2)}}\,||M||^{r-2}\,||M^{-1}||^{3/2}\,||M^{-1}||^{r+2}\\ &\quad\times||M||^{3/2}||\nabla_h\times\mathbf{E}||_{r+1,\omega,\Omega}\\ &\leq C\,\rho^{r/2-1/4}\,(\omega^{-5/2}+\omega^{-4})\frac{h^{r-2}}{m^{\theta\lambda(r-3/2)}}||\nabla_h\times\mathbf{E}||_{r+1,\omega,\Omega}.\end{aligned}\tag{5.33}$$

This completes the proof. □

Remark 5.1. In the considered anisotropic case, the derived error estimates contain a factor depending on the condition number ρ of the coefficient matrix. Under the quasi-uniformity assumption, we believe that the orders of the condition number ρ in the error estimates are optimal in the sense that the transformation estimates are sharp. Numerical experiments yet indicate that there may be room for improvement in the final estimates, which would probably need a completely new proof strategy. The other dependencies on the mesh size h and the number p of wave directions are the same as that in [8]. Besides, if one does not use the transformation back and forth to the isotropic case, namely, anisotropic plane waves are employed, we can not prove the corresponding error estimates owing to the absence of the revelent approximation properties of anisotropic plane waves (see [15, p.351]).

6 Local-global variational formulation for the nonhomogeneous and anisotropic Maxwell equations

In this section we shall describe a PWDG-LSFE method, which is similar to the PWLS-LSFE method proposed in [12], to discretize the nonhomogeneous and anisotropic Maxwell's equations.

6.1 A PWDG-LSFE method

Consider three-dimensional nonhomogeneous and anisotropic Maxwell's equations written as a first-order system of equations:

$$\begin{cases}\nabla\times\mathbf{E}-i\omega\mu\mathbf{H}=\mathbf{0},\\ \nabla\times\mathbf{H}+i\omega\varepsilon\mathbf{E}=\mathbf{J},\end{cases}\quad\text{in }\ \Omega,\tag{6.1}$$

with the lowest-order absorbing boundary condition (2.3). We need to transform nonhomogeneous problems into homogeneous problems to use the PWDG method.

By using the above equations, we obtain the second-order nonhomogeneous Maxwell equations

$$\begin{cases} \nabla\times\Big(\dfrac{1}{i\omega}\mu^{-1}\nabla\times\mathbf{E}\Big)+i\omega\varepsilon\mathbf{E}=\mathbf{J}, & \text{in } \Omega, \\ (\mu^{-1}\nabla\times\mathbf{E})\times\mathbf{n}-i\omega\vartheta(\mathbf{n}\times\mathbf{E})\times\mathbf{n}=\mathbf{g}, & \text{on } \gamma. \end{cases} \tag{6.2}$$

We assume that $\mathbf{J}$ is defined in a slightly large domain containing Ω as its subdomain and decompose the solution $\mathbf{E}$ of the problem (6.2) into $\mathbf{E}=\mathbf{E}^{(1)}+\mathbf{E}^{(2)}$, where $\mathbf{E}^{(1)}$ is a piecewise particular solution of Eq. (6.2) without the primal boundary condition, and $\mathbf{E}^{(2)}$ locally satisfies the homogeneous Maxwell equations.

We use the same idea in [12]. For each element Ω_k, let Ω_k^* be a fictitious domain that has almost the same size as Ω_k and contains Ω_k as its subdomain. The particular solution $\mathbf{E}^{(1)}\in(L^2(\Omega))^3$ is defined as $\mathbf{E}^{(1)}|_{\Omega_k}=\mathbf{E}_k^{(1)}|_{\Omega_k}$ for each Ω_k, where $\mathbf{E}_k^{(1)}\in H(\text{curl};\Omega_k^*)$ satisfies the nonhomogeneous *local* Maxwell equations on the fictitious domain Ω_k^*:

$$\nabla\times\Big(\frac{1}{i\omega}\mu^{-1}\nabla\times\mathbf{E}_k^{(1)}\Big)+i\omega\varepsilon\mathbf{E}_k^{(1)}=\mathbf{J} \quad \text{in} \quad \Omega_k^* \ (k=1,2,\cdots,N) \tag{6.3}$$

with the homogeneous boundary condition

$$\big(\mu^{-1}\nabla\times\mathbf{E}_k^{(1)}\big)\times\mathbf{n}-i\omega\vartheta\big(\mathbf{n}\times\mathbf{E}_k^{(1)}\big)\times\mathbf{n}=\mathbf{0} \quad \text{on} \quad \partial\Omega_k^*. \tag{6.4}$$

The variational problem of $(6.3)-(6.4)$ is: to find $\mathbf{E}_k^{(1)}\in H(\text{curl},\Omega_k^*)$ such that

$$\begin{cases} \displaystyle\int_{\Omega_k^*}\Big(\frac{1}{i\omega}\mu^{-1}\nabla\times\mathbf{E}_k^{(1)}\cdot\nabla\times\bar{\mathbf{F}}_k+i\omega\varepsilon\mathbf{E}_k^{(1)}\cdot\bar{\mathbf{F}}_k\Big)d\mathbf{x}+\int_{\partial\Omega_k^*}\vartheta(\mathbf{E}_k^{(1)}\times\mathbf{n})\times\mathbf{n}\cdot\bar{\mathbf{F}}_k dS \\ \displaystyle\quad=\int_{\Omega_k^*}\mathbf{J}\cdot\bar{\mathbf{F}}_k d\mathbf{x}, \quad \forall\mathbf{F}_k\in\mathrm{H}(\text{curl},\Omega_k^*) \ \ (k=1,2,\cdots,N). \end{cases} \tag{6.5}$$

When $\mathbf{J}$ satisfies $\mathbf{J}\in(L^2(\Omega_k^*))^3$, the variational problem (6.5) possesses a unique solution $\mathbf{E}_k^{(1)}\in H(\text{curl},\Omega_k^*)$ (see [21, Chap 4]).

Let q be a positive integer and D be a bounded and connected domain in $\mathbf{R}^3$. Let $S_q(D)$ denote the set of polynomials defined on D, whose orders are less or equal to q. Set $\mathbf{S}_q(D)=(S_q(D))^3$.

The discrete variational problem of Eq. (6.5) is: to find $\mathbf{E}_{k,h}^{(1)}\in\mathbf{S}_q(\Omega_k^*)$ such that

$$\begin{cases} \displaystyle\int_{\Omega_k^*}\Big(\frac{1}{i\omega}\mu^{-1}\nabla\times\mathbf{E}_{k,h}^{(1)}\cdot\nabla\times\bar{\mathbf{F}}_k+i\omega\varepsilon\mathbf{E}_{k,h}^{(1)}\cdot\bar{\mathbf{F}}_k\Big)d\mathbf{x}+\int_{\partial\Omega_k^*}\frac{1}{\sigma}\big(\mathbf{E}_{k,h}^{(1)}\times\mathbf{n}\big)\times\mathbf{n}\cdot\bar{\mathbf{F}}_k d\mathbf{x} \\ \displaystyle\quad=\int_{\Omega_k^*}\mathbf{J}\cdot\bar{\mathbf{F}}_k d\mathbf{x}, \quad \forall\mathbf{F}_k\in\mathbf{S}_q(\Omega_k^*) \ \ (k=1,2,\cdots,N). \end{cases} \tag{6.6}$$

In this paper we choose the fictitious domain Ω_k^* to be the sphere for the three-dimensional case (see Remark 2.1 in [12]). Then the variational problems (6.6) can be solved easily by using the polar coordinate transformation for the calculation of the involved integrations. Define $\mathbf{E}_h^{(1)}\in\prod_{k=1}^N \mathbf{S}_q(\Omega_k)$ by $\mathbf{E}_h^{(1)}|_{\Omega_k}=\mathbf{E}_{k,h}^{(1)}|_{\Omega_k}$.

It is easy to see that $\mathbf{E}^{(2)}=\mathbf{E}-\mathbf{E}^{(1)}$ is uniquely determined by the following homogeneous Maxwell equations of $\mathbf{E}_k^{(2)}$ $(=\mathbf{E}^{(2)}|_{\Omega_k})$:

$$\nabla\times\Big(\frac{1}{i\omega}\mu^{-1}\nabla\times\mathbf{E}_k^{(2)}\Big)+i\omega\varepsilon\mathbf{E}_k^{(2)}=\mathbf{0}\quad\text{in}\quad\Omega_k\ (k=1,2,\cdots,N)\tag{6.7}$$

with the following boundary condition on γ and the interface conditions on Γ_{lj} $(l<j;\ l,j=1,\cdots,N)$:

$$\begin{aligned}&\frac{1}{i\omega}(\mu^{-1}\nabla\times\mathbf{E}^{(2)})\times\mathbf{n}-\vartheta(\mathbf{n}\times\mathbf{E}^{(2)})\times\mathbf{n}\\&=\mathbf{g}/i\omega-\frac{1}{i\omega}(\mu^{-1}\nabla\times\mathbf{E}^{(1)})\times\mathbf{n}+\vartheta(\mathbf{n}\times\mathbf{E}^{(1)})\times\mathbf{n}\quad\text{on}\ \gamma,\\&(\mu^{-1}\nabla\times\mathbf{E}_l^{(2)})\times\mathbf{n}_l+(\mu^{-1}\nabla\times\mathbf{E}_j^{(2)})\times\mathbf{n}_j\\&=-\Big((\mu^{-1}\nabla\times\mathbf{E}_l^{(1)})\times\mathbf{n}_l+(\mu^{-1}\nabla\times\mathbf{E}_j^{(1)})\times\mathbf{n}_j\Big)\quad\text{on}\ \Gamma_{lj},\\&\mathbf{E}_l^{(2)}\times\mathbf{n}_l+\mathbf{E}_j^{(2)}\times\mathbf{n}_j=-\Big(\mathbf{E}_l^{(1)}\times\mathbf{n}_l+\mathbf{E}_j^{(1)}\times\mathbf{n}_j\Big)\quad\text{on}\ \Gamma_{lj}.\end{aligned}\tag{6.8}$$

As in the derivation of the PWDG method stated in Section 3, we can derive the simplified variational problem of $\mathbf{E}_h^{(2)}$: find $\mathbf{E}_h^{(2)}\in\mathbf{V}_p(\mathcal{T}_h)$ such that

$$\mathcal{A}_h(\mathbf{E}_h^{(2)},\boldsymbol{\xi}_{h,p})=\ell_h(\boldsymbol{\xi}_{h,p}),\quad\forall\boldsymbol{\xi}_{h,p}\in\mathbf{V}_p(\mathcal{T}_h),\tag{6.9}$$

where

$$\begin{aligned}\ell_h(\boldsymbol{\xi})=&\,i\omega\sum_k\int_{\Omega_k}\mathbf{J}\cdot\overline{\boldsymbol{\xi}}\,d\mathbf{x}-\mathcal{A}_h(\mathbf{E}_h^{(1)},\boldsymbol{\xi})\\&-i\omega^{-1}\int_{\mathcal{F}_h^{\mathrm{B}}}\delta\vartheta^{-1}(\mathbf{n}\times\mathbf{g})\cdot\overline{\mu_r^{-1}\nabla_h\times\boldsymbol{\xi}}\,dS+\int_{\mathcal{F}_h^{\mathrm{B}}}(1-\delta)(\mathbf{n}\times\mathbf{g})\cdot\overline{(\mathbf{n}\times\boldsymbol{\xi})}\,dS.\end{aligned}\tag{6.10}$$

6.2 Error estimates in mesh-skeleton norm

By using the transformations (2.4) and (2.9), the scaled electric and magnetic fields $(\hat{\mathbf{E}},\hat{\mathbf{H}})$ satisfy the following nonhomogeneous Maxwell equations

$$\begin{cases}\nabla\times\hat{\mathbf{E}}-i\omega\mu_r\hat{\mathbf{H}}=\mathbf{0},\\\nabla\times\hat{\mathbf{H}}+i\omega\varepsilon_r\hat{\mathbf{E}}=\tilde{M}^{-1}\,\mathbf{J},\end{cases}\quad\text{in}\ \hat{\Omega}.\tag{6.11}$$

For ease of notation, we set

$$\mathcal{F}(u,f,s)=||u||_{s,\omega,\Omega}+\sum_{l=0}^{s-2}\omega^{s-l-2}||f||_{l,\Omega_\delta}.$$

Then we have the following convergence results.

Theorem 6.1. *Assume that the analytical solution* $\mathbf{E}\in H^s(curl;\Omega)$ *($s\in\mathbf{N}$) satisfies the non-homogeneous and anisotropic Maxwell equations* (6.1) *with the boundary condition* (2.3). *Let* $\mathbf{E}_h=\mathbf{E}_h^{(1)}+\mathbf{E}_h^{(2)}\in\prod_{k=1}^N\mathbf{S}_q(\Omega_k)+\mathbf{V}_p(\mathcal{T}_h), p=(m+1)^2$ *with* $q\geq 2$ *and* $2\leq s\leq\min\{(m+1)/2,q+1\}$ *be the approximation defined by* (6.6) *and* (6.9). *Then there exists a constant C independent of p but depending on ω and h through the product ωh as an increasing function, such that, for large p,*

$$|||\mathbf{E}-\mathbf{E}_h|||_{\mathcal{F}_h}\leq C\,\rho^{s/2+1}\,h^{s-3/2}(\omega^{-1/2}m^{-\theta\lambda(s-5/2)}+\omega^{1/2}q^{-(s-3/2)})\mathcal{F}(\nabla\times\mathbf{E},\mathbf{J},s), \tag{6.12}$$

where $C=C(\omega h)>0$ *depends on the shape of the* $\Omega_k\in\mathcal{T}_h,r,\vartheta,\varepsilon,\mu$ *and on the flux parameters, and* $\theta>0$ *depends on the coordinate transformation matrix M.*

Proof. By Lemma 5.3, and using the transformations (2.4) and (2.9), we deduce that

$$|||\mathbf{E}-\mathbf{E}_h|||_{\mathcal{F}_h}\leq C\,\rho\,|||\hat{\mathbf{E}}-\hat{\mathbf{E}}_{\hat{h}}|||_{\hat{\mathcal{F}}_{\hat{h}}}. \tag{6.13}$$

By Theorem 4.8 of [12], we can show that

$$|||\hat{\mathbf{E}}-\hat{\mathbf{E}}_{\hat{h}}|||_{\hat{\mathcal{F}}_{\hat{h}}}\leq C\,\rho\,\hat{h}^{s-3/2}(\omega^{-1/2}m^{-\hat{\lambda}(s-5/2)}+\omega^{1/2}q^{-(s-3/2)})\mathcal{F}(\nabla_{\hat{h}}\times\hat{\mathbf{E}},\tilde{M}^{-1}\,\mathbf{J},s). \tag{6.14}$$

Notice that $\hat{h}\leq C\,||M||\,h$ and

$$\begin{aligned}
&\mathcal{F}(\nabla_{\hat{h}}\times\hat{\mathbf{E}},\tilde{M}^{-1}\,\mathbf{J},s)=||\nabla_{\hat{h}}\times\hat{\mathbf{E}}||_{s,\omega,\hat{\Omega}}+\sum_{l=0}^{s-2}\omega^{s-l-2}||\tilde{M}^{-1}\,\mathbf{J}||_{l,\hat{\Omega}_\delta}\\
&=||\tilde{M}^{-1}(\nabla_h\times\mathbf{E})||_{s,\omega,\hat{\Omega}}+\sum_{l=0}^{s-2}\omega^{s-l-2}||\tilde{M}^{-1}\,\mathbf{J}||_{l,\hat{\Omega}_\delta}\\
&\leq C\Big(||M||^{3/2}\,||M^{-1}||^{s+1}||\nabla_h\times\mathbf{E}||_{s,\omega,\Omega}+\sum_{l=0}^{s-2}\omega^{s-l-2}||M||^{3/2}\,||M^{-1}||^{l+1}||\mathbf{J}||_{l,\Omega_\delta}\Big).
\end{aligned}$$

Substituting the above inequality into (6.14), together with (6.13), yields

$$\begin{aligned}
|||\mathbf{E}-\mathbf{E}_h|||_{\mathcal{F}_h}&\leq C\,\rho\,h^{s-3/2}\big(\omega^{-1/2}m^{-\theta\lambda(s-5/2)}+\omega^{1/2}q^{-(s-3/2)}\big)\\
&\quad\times\left(||M||^s\,||M^{-1}||^{s+1}||\nabla_h\times\mathbf{E}||_{s,\omega,\Omega}+\sum_{l=0}^{s-2}\omega^{s-l-2}||M||^s\,||M^{-1}||^{l+1}||\mathbf{J}||_{l,\Omega_\delta}\right)\\
&\leq C\,\rho^{s/2+1}\,h^{s-3/2}(\omega^{-1/2}m^{-\theta\lambda(s-5/2)}+\omega^{1/2}q^{-(s-3/2)})\mathcal{F}(\nabla_h\times\mathbf{E},\mathbf{J},s).
\end{aligned}$$

This completes the proof. □

7 Numerical experiments

In this section we apply the PWDG method to solve electromagnetic wave propagation in anisotropic media, and we report some numerical results to verify the efficiency of the proposed method. Besides, we give the comparison of the accuracy between the PWDG and the PWLS in numerical experiments.

For the examples discussed in this section, we adopt a uniform triangulation $\mathcal{T}_h$ for the domain Ω as follows. Ω is divided into small cubes for three-dimensional case. As described in Sections 3 and 4, we choose the same number p of basis functions for every elements Ω_k.

We consider the choice of numerical fluxes for the PWDG method: with constant parameters, as in the original ultra weak variational formulation (UWVF) introduced in [3] $(\alpha=\beta=\delta=1/2)$. We only assume that $\varepsilon_r=\mu_r=1$.

To measure the accuracy of the numerical solution $\mathbf{E}_h$, we introduce the following L^2 relative error:

$$\text{err.}=\frac{||\mathbf{E}-\mathbf{E}_h||_{L^2(\Omega)}}{||\mathbf{E}||_{L^2(\Omega)}}$$

for the exact solution $\mathbf{E}\in(L^2(\Omega))^3$.

7.1 Electric dipole in free space for a smooth case

We compute the electric field due to an electric dipole source at the point $\mathbf{x}_0=(-0.6,-0.6,-0.6)$. The dipole point source can be defined as the solution of a homogeneous Maxwell system (2.2). The exact solution of the problems is

$$\mathbf{E}_{\text{ex}}=-\mathrm{i}\omega I\phi(\mathbf{x},\mathbf{x}_0)G\,\mathbf{a}+\frac{I}{\mathbf{i}\omega\varepsilon_r}G\,\nabla_{\hat{h}}(\nabla_{\hat{h}}\phi\cdot\mathbf{a}), \tag{7.1}$$

where

$$\phi(\mathbf{x},\mathbf{x}_0)=\frac{\exp\left(\mathrm{i}\omega\sqrt{\varepsilon_r}\left|M\,\mathbf{x}-\mathbf{x}_0\right|\right)}{4\pi\left|M\,\mathbf{x}-\mathbf{x}_0\right|}$$

and $\Omega=[0,1]^3$. To keep the exact solution smooth in Ω, the singularity $\mathbf{x}_0$ is not equal to $M\,\mathbf{x}$ where $\mathbf{x}\in\Omega$.

At first we set $\omega=4\pi$ and $\Lambda=\text{diag}(1,1,0.5)$. Table 1 shows the errors with respect to p of the approximations generated by the PWDG method in $|||\cdot|||_{\mathcal{F}_h}$-norm and relative L^2-norm, respectively. A fairly coarse mesh $h=1/4$ is used, we choose the number p of basis functions from $p=9$ to $p=64$ $(2\leq m\leq 7)$.

Fig. 1 shows the plot of $|||\mathbf{E}-\mathbf{E}_h|||_{\mathcal{F}_h}$ and L^2 relative errors with respect to m, respectively. It highlights two different regimes for increasing m: (i) a preasymptotic region with slow convergence, (ii) a region of faster convergence. As stated in Remark 3.14 (see [7]),

Table 1: $\mathcal{F}_h$-norm errors of the approximations for the case of p-convergence.

p	9	16	25	36	49	64
$\|\|\|\mathbf{E}-\mathbf{E}_h\|\|\|_{\mathcal{F}_h}$	5.86e-1	1.94e-1	4.95e-2	1.05e-2	1.45e-3	2.08e-4
err.	3.64e-1	7.60e-2	1.94e-2	4.78e-3	6.13e-4	8.13e-5

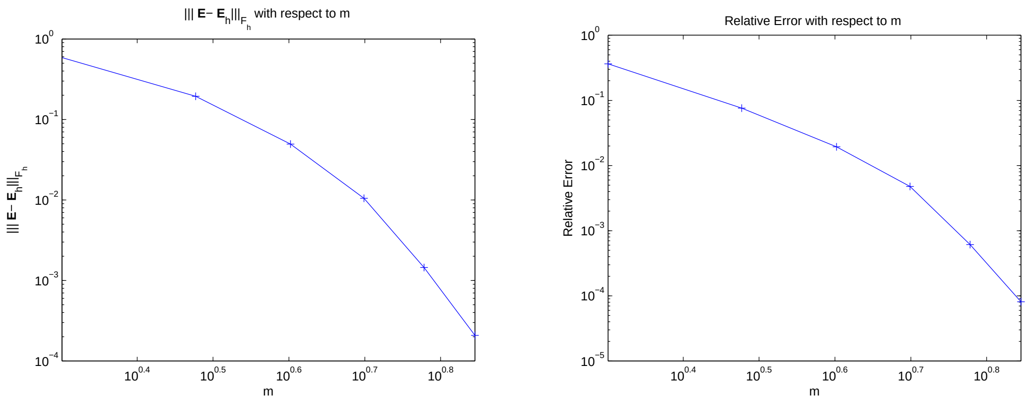

Figure 1: Left: $|||\mathbf{E}-\mathbf{E}_h|||_{\mathcal{F}_h}$ vs m. Right: $Err.$ vs m.

the convergence order of the approximations with respect to m turns out to be exponential since the analytical solution of the problem can be extended analytically outside the domain.

We fix the number of the plane wave basis functions as $p=25$, but decrease the mesh size h. The resulting relative L^2 errors of the approximations generated by the PWDG method are listed in Table 2 and Fig. 2.

Fig. 2 shows the errors of the numerical solutions in $|||\cdot|||_{\mathcal{F}_h}$-norm and relative L^2-norm with respect to h in logarithmic scale, respectively. As stated in [6, Sect. 5], we observe the algebraic convergence in terms of h for $p=25$.

We fix $\omega h=\pi/2$, but decrease the mesh size h and increase the wave number ω. The resulting errors of the approximations generated by the PWDG and the PWLS are listed in Table 3 and Fig. 3.

Table 3 and Fig. 3 show that from the viewpoint of the relative L^2 errors, the approximations generated by the PWDG are more accurate than those generated by the PWLS. Besides, the numerical errors in relative L^2-norm indicate that the PWDG method may not be affected by the pollution effect (see [35]) when ωh and p are fixed.

We fix $\omega=2\pi, h=1/4, p=36$, but increase the condition number of the anisotropic matrix $\Lambda=\mathrm{diag}(1.0,1.0,2^{id})$, $1\leq id\leq 6$, where the third element on the diagonal are monotonically increasing. The resulting errors of the approximations generated by the PWDG and the PWLS are listed in Table 4 and Fig. 4.

We can see from Table 4 and Fig. 4 that from the viewpoint of the relative L^2 errors, the approximations generated by the PWDG are more accurate than those generated by

Table 2: Errors of approximations with respect to h. ($p=25$).

h	1/4	1/6	1/8	1/10	1/12
$\|\|\|\mathbf{E}-\mathbf{E}_h\|\|\|_{\mathcal{F}_h}$	4.95e-2	1.26e-2	4.62e-3	2.11e-3	1.10e-3
err.	1.94e-2	4.23e-3	1.42e-3	6.05e-4	3.02e-4

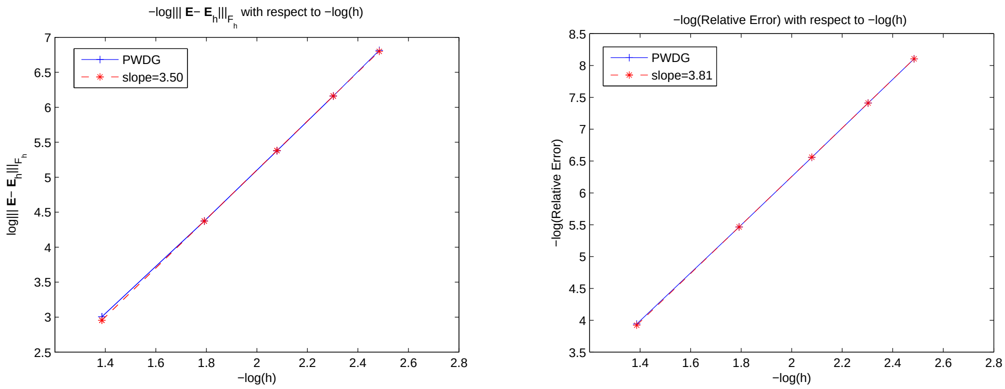

Figure 2: Left: $-\log(|||\mathbf{E}-\mathbf{E}_h|||_{\mathcal{F}_h})$ vs $-\log(h)$. Right: $-\log(Err.)$ vs $-\log(h)$.

Table 3: Errors of approximations with respect to h ($\omega h=\pi/2$, $p=25$).

	ω	2π	3π	4π	5π	6π	7π	8π
PWDG	$\|\|\|\mathbf{E}-\mathbf{E}_h\|\|\|_{\mathcal{F}_h}$	2.14e-3	3.26e-3	4.62e-3	6.24e-3	8.12e-3	1.02e-2	1.26e-2
	err.	2.07e-3	1.66e-3	1.42e-3	1.27e-3	1.17e-3	1.10e-3	1.05e-3
PWLS	$\|\|\|\mathbf{E}-\mathbf{E}_h\|\|\|_{\mathcal{F}_h}$	1.97e-3	2.90e-3	4.03e-3	5.37e-3	6.93e-3	8.73e-3	1.08e-2
	err.	2.80e-3	2.53e-3	2.29e-3	2.11e-3	1.99e-3	1.89e-3	1.81e-3

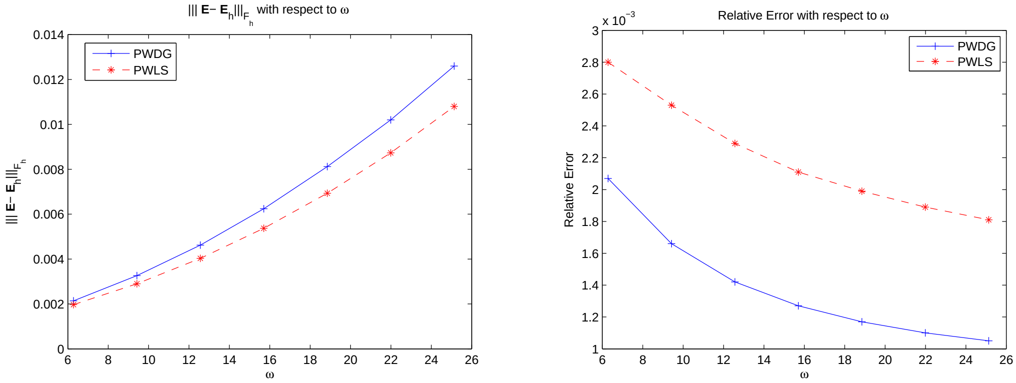

Figure 3: Left: $|||\mathbf{E}-\mathbf{E}_h|||_{\mathcal{F}_h}$ vs ω. Right: $Err.$ vs ω.

Table 4: Errors of approximations with respect to cond(Λ) ($\omega=2\pi$, $p=36$, $h=1/4$).

	cond(Λ)	2	4	8	16	32	64
PWDG	$\lvert\lvert\lvert \mathbf{E}-\mathbf{E}_h \rvert\rvert\rvert_{\mathcal{F}_h}$	1.15e-3	3.22e-3	9.25e-3	2.51e-2	5.99e-2	9.01e-2
	err.	1.64e-3	4.95e-3	1.59e-2	6.04e-2	2.45e-1	6.52e-1
PWLS	$\lvert\lvert\lvert \mathbf{E}-\mathbf{E}_h \rvert\rvert\rvert_{\mathcal{F}_h}$	1.06e-3	2.95e-3	8.81e-3	2.61e-2	6.15e-2	8.71e-2
	err.	1.74e-3	5.40e-3	2.05e-2	1.04e-1	3.88e-1	7.39e-1

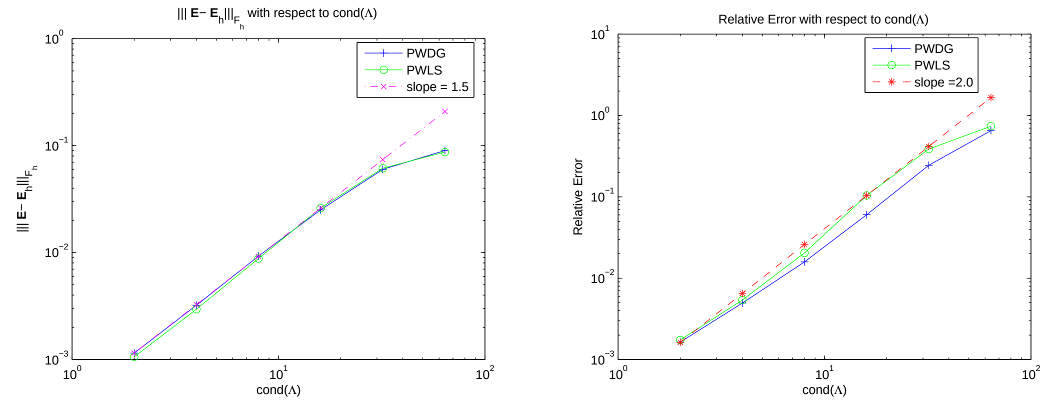

Figure 4: Left: $\lvert\lvert\lvert \mathbf{E}-\mathbf{E}_h \rvert\rvert\rvert_{\mathcal{F}_h}$ vs cond(Λ). Right: $Err.$ vs cond(Λ).

the PWLS. Besides, the figure displays a linear plot, which indicates that the accuracies of the approximations are indeed affected by the condition number of the anisotropic matrix Λ. In particular, according to Theorem 5.1, the number r in the error estimate (5.29) is equal to $r=(m-1)/2=2$ $(m=5)$, which means that the theoretical convergence order is $r/2+1=2$. Moreover, the numerical convergence order, i.e., the slope of the line in Fig. 4 (left) is 1.5, which is superior to the theoretical order.

7.2 A nonhomogeneous Maxwell's equations in three dimensions

We consider the following analytical solution

$$\mathbf{E}_{\rm ex}=\omega(xz\,\cos y,-z\,\sin y,xy)^t. \tag{7.2}$$

The source term $\mathbf{J}$ determined by the above solution does not vanish over the entire computational domain $[0,1]^3$. The discretization of the underlying equations is the same as that of the equations described in Section 6.

We set $\omega=2\pi$ and choose the number p of the plane wave basis functions as $p=16$. Then we report the results of the PWDG-LSFE method when h decreases. Table 5 and Fig. 5 show the $\lvert\lvert\lvert\cdot\rvert\rvert\rvert_{\mathcal{F}_h}$-norm errors and relative L^2 errors of the approximations.

Fig. 5 shows the errors of the numerical solutions in $\lvert\lvert\lvert\cdot\rvert\rvert\rvert_{\mathcal{F}_h}$-norm and relative L^2-norm with respect to h in logarithmic scale, respectively. It displays a linear plot which

Table 5: Errors of approximations with respect to h and q $(\omega=2\pi,\ p=16)$.

	h	$1/3$	$1/4$	$1/5$	$1/6$	$1/7$	$1/8$
$q=2$	$\|\|\|\mathbf{E}-\mathbf{E}_h\|\|\|_{\mathcal{F}_h}$	1.08	5.13e-1	2.94e-1	1.85e-1	1.25e-1	8.87e-2
	err.	5.59e-2	2.72e-2	1.59e-2	1.02e-2	7.03e-3	5.12e-3
$q=3$	$\|\|\|\mathbf{E}-\mathbf{E}_h\|\|\|_{\mathcal{F}_h}$	6.13e-1	3.44e-1	2.15e-1	1.46e-1	1.05e-1	7.88e-2
	err.	2.52e-2	9.94e-3	4.98e-3	2.80e-3	1.73e-3	1.14e-3

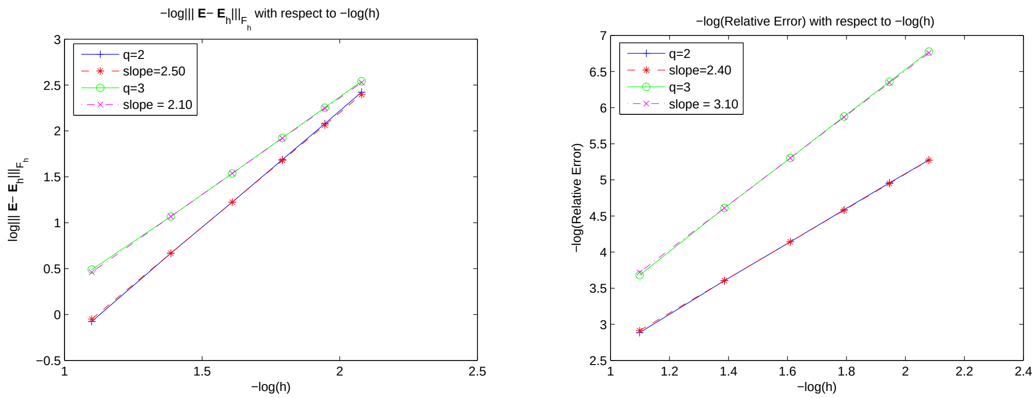

Figure 5: Left: $-\log(|||\mathbf{E}-\mathbf{E}_h|||_{\mathcal{F}_h})$ vs $-\log(h)$. Right: $-\log(Err.)$ vs $-\log(h)$.

verifies the validity of the theoretical results in Theorem 6.1. According to Theorem 6.1, the number s defining the h-convergence orders in the error estimate (6.12) is $\min\{(m+1)/2,q+1\}=2$, which implies that the $|||\cdot|||_{\mathcal{F}_h}$-norm errors have only 0.5-order convergence with respect to h (for a fixed ω). Fortunately, the plots indicate that $|||\cdot|||_{\mathcal{F}_h}$-norm errors possess about 2-order convergence with respect to h, which is obviously superior to the theoretical results. We point out that, for the case of homogeneous equations, the numerical h-convergence order in $|||\cdot|||_{\mathcal{F}_h}$-norm is also higher than the theoretical h-convergence order (see Remarks 4.12 and 4.15 in [6] and the numerical results reported in [10]), which indicates that the approximation estimate given in Lemma 5.4 might be improved.

We fix $\omega h=\pi/2$, but decrease the mesh size h and increase the wave number ω. The resulting errors of the approximations generated by the PWDG-LSFE and the PWLS-LSFE are listed in Table 6 and Fig. 6.

Table 6 and Fig. 6 show that the approximations generated by the PWDG-LSFE and the PWLS-LSFE almost have the same accuracy in $|||\cdot|||_{\mathcal{F}_h}$-norm and relative L^2-norm. Besides, the numerical errors in relative L^2-norm indicate that the PWDG-LSFE and the PWLS-LSFE are slightly affected by the pollution effect.

We fix $\omega=2\pi,h=1/4,p=16$, but increase the condition number of the anisotropic matrix $\Lambda=\mathrm{diag}(1.0,1.0,1/2^{id})$, where id is chosen from 1 to 10. The resulting errors of the approximations generated by the PWDG-LSFE and the PWLS-LSFE are listed in Fig. 7.

We can see from Fig. 7 that the approximations generated by the PWDG-LSEF and

Table 6: Errors of approximations with respect to h ($\omega h = \pi/2$, $q=2$).

	ω	2π	3π	4π	5π	6π	7π
PWDG	$\|\|\|\mathbf{E}-\mathbf{E}_h\|\|\|_{\mathcal{F}_h}$	5.13e-1	7.88e-1	1.14	1.58	1.98	2.59
	err.	2.72e-2	2.92e-2	2.76e-2	2.68e-2	2.73e-2	2.60e-2
PWLS	$\|\|\|\mathbf{E}-\mathbf{E}_h\|\|\|_{\mathcal{F}_h}$	5.08e-1	7.80e-1	1.12	1.54	1.91	2.48
	err.	2.70e-2	2.90e-2	2.69e-2	2.61e-2	2.59e-2	2.45e-2

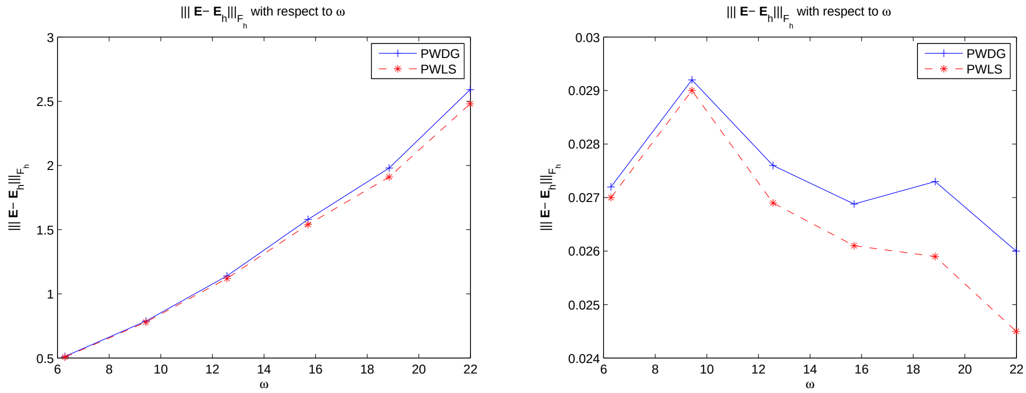

Figure 6: Left: $|||\mathbf{E}-\mathbf{E}_h|||_{\mathcal{F}_h}$ vs ω. Right: $Err.$ vs ω.

the PWLS-LSFE are comparable in the accuracy. The numerical convergence order with respect to the condition number of the matrix Λ for the PWDG-LSFE method in $|||\cdot|||_{\mathcal{F}_h}$-norm are obviously superior to the theoretical results in Theorem 6.1. For example, we investigate the convergence order of the $|||\cdot|||_{\mathcal{F}_h}$-norm errors with respect to the condition number. According to Theorem 6.1, the number s in the error estimate (6.12) is equal to $s = \min\{(m+1)/2, q+1\} = 3$, which means that the theoretical convergence order is $s/2+1 = 2.5$ (for a fixed ω). However, the numerical convergence order, i.e., the slope of the line in Fig. 7 (left) is 1.0, which is obviously superior to the theoretical order.

8 Conclusion

In this paper we have introduced a plane-wave discontinuous Galerkin method for discretization of the three-dimensional time-harmonic anisotropic (homogeneous and nonhomogeneous) Maxwell equations with the diagonal matrix coefficients in anisotropic media, and derived error estimates of the resulting approximate solutions. We reported some numerical results to illustrate that the approximate solutions generated by the new method possess high accuracy, and verify the validity of the theoretical results.

The current error estimates of the PWDG (and other plane wave methods) are obtained for the case of the diagonal matrix coefficients only, and there are new difficul-

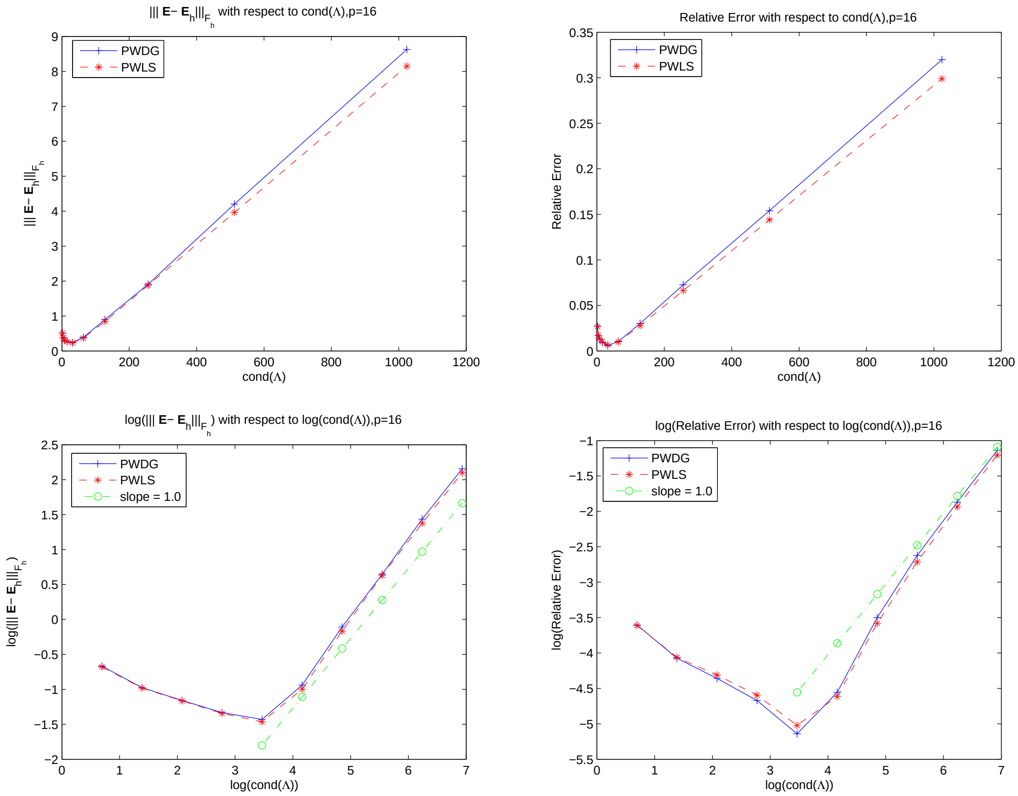

Figure 7: Top (left): $|||\mathbf{E}-\mathbf{E}_h|||_{\mathcal{F}_h}$ vs ρ, Top (right): $Err.$ vs ρ; Bottom (left): $\log(|||\mathbf{E}-\mathbf{E}_h|||_{\mathcal{F}_h})$ vs $\log(\rho)$, Bottom (right): $\log(Err.)$ vs $\log(\rho)$.

ties in the theoretical analysis of the PWDG (and other plane wave methods) for the three-dimensional anisotropic Maxwell equations with the general matrix coefficients. In future work, we will give error analysis for the general case of the non-diagonal matrix coefficients.

Acknowledgments

The first author was supported by China NSF under the grant 11501529, Qinddao applied basic research project under grant 17-1-1-9-jch and Scientific Research Foundation of Shandong University of Science and Technology for Recruited Talents. The second author was supported by the Natural Science Foundation of China G11571352.

References

[1] W. Cao, D. Li and Z. Zhang, Optimal Superconvergence of Energy Conserving Local Discontinuous Galerkin Methods for Wave Equations, Commun. Comput. Phys., 21(2017), 211-236.

[2] O. Cessenat, Application d'une nouvelle formulation variationnelle aux équations d'ondes harmoniques, Problèmes de Helmholtz 2D et de Maxwell 3D, Ph.D. Thesis, Université Paris IX Dauphine, 1996.

[3] O. Cessenat and B. Despres, Application of an ultra weak variational formulation of elliptic pdes to the two-dimensional Helmholtz problem, SIAM J. Numer. Anal. 35(1998), 255-299.

[4] O. Cessenat and B. Despres, Using plane waves as basis functions for solving time harmonic equations with the ultra weak variational formulation, J. Comput. Acous., 11(2003), 227-238.

[5] G. Gabard, Discontinuous Galerkin methods with plane waves for time-harmonic problems, J. Comput. Phys., 225 (2007), 1961-1984.

[6] C. Gittelson, R. Hiptmair and I. Perugia, Plane wave discontinuous Galerkin methods: Analysis of the h-version, ESAIM: M2AN Math. Model. Numer. Anal., 43(2009), 297-331.

[7] R. Hiptmair, A. Moiola, and I. Perugia, Plane wave discontinuous Galerkin methods for the 2D Helmholtz equation: analysis of the p-version. SIAM J. Numer. Anal., 49(2011), 264-284.

[8] R. Hiptmair, A. Moiola, and I. Perugia, Error analysis of Trefftz-discontinuous Galerkin methods for the time-harmonic Maxwell equations, Math. Comp., 82(2013), 247-268.

[9] R. Hiptmair, A. Moiola, and I. Perugia, A survey of Trefftz for the Helmholtz equation, Springer Lecture Notes 114, 2016.

[10] Q. Hu and L. Yuan, A weighted variational formulation based on plane wave basis for discretization of Helmholtz equations, Int. J. Numer. Anal. Model., 11(2014), 587-607.

[11] Q. Hu and L. Yuan, A Plane Wave Least-Squares Method for Time-Harmonic Maxwell's Equations in Absorbing Media, SIAM J. Sci. Comput., 36(2014), A1911-A1936.

[12] Q. Hu and L. Yuan, A Plane wave method combined with local spectral elements for nonhomogeneous Helmholtz equation and time-harmonic Maxwell equations, Adv. Comput. Math., 44(2018), 245-275.

[13] Q. Hu and L. Zhao, A Two-Steps Method Based on Plane Wave for Nonhomogeneous Helmholtz Equations in Inhomogeneous Media, Numer. Math. Theor. Meth. Appl., 11 (2018), 453-476.

[14] T. Huttunen, M. Malinen, P. Monk, Solving Maxwell's equations using the ultra weak variational formulation, J. Comput. Phys., 223 (2007), 731-758.

[15] T. Huttunen and P. Monk, The use of plane waves to approximate wave propagation in anisotropic media, J. Comp. Math., 25(2007), 350-367.

[16] T. Huttunen and P. Monk, F. Collino and J. Kaipio, The ultra-weak variational formulation for elastic wave problems, SIAM J. Sci. Comput., 25(2004), 1717-1742.

[17] T. Luostari, T. Huttunen and P. Monk, Error estimates for the ultra weak variational formulation in linear elasticity, ESAIM: M2AN Math. Model. Numer. Anal., 47(2013), 183-211.

[18] R. Marqués, F. Medina, and R. Rafii-El-Idrissi, Role of bianisotropy in negative permeability and left-handed metamaterials, Phys. Rev. B, 65(2002), 144440-144440.

[19] L. Mei, C. Liu and X. Wu, Runge-Kutta-Nystrom Integrators when Applied to Nonlinear Wave Equations, Commun. Comput. Phys., 22(2017), 742-764.

[20] A. Moiola, R. Hiptmair, and I. Perugia, Plane wave approximation of homogeneous Helmholtz solutions, Z. Angew. Math. Phys., 62(2011), 809-837.

[21] P. Monk, Finite element methods for Maxwell's equation, Oxford University Press, 2003.

[22] P. Monk and D. Wang, A least-squares method for the Helmholtz equation, Comput. Meth. Appl. Mech. Engng., 175(1999), 121-136.

[23] H. Riou, P. Ladevèze, B. Sourcis, The multiscale VTCR approach applied to acoustics problems, J. Comput. Acous., 16(2008), 487-505.

[24] H. Riou, P. Ladevèze, B. Sourcis, B. Faverjon and L. Kovalevsky, An adaptive numerical strat-

egy for the media-frequency analysis of Helmholtz's problem, J. Comput. Acous., 20(2012), DOI: 10.1142/S0218396X11004481.

[25] Z. Sacks, D. Kingsland, R. Lee and J. Lee, A perfectly matched anisotropic absorber for use an absorbing boundary condition, IEEE Trans. Antennas Propagat., 43(1995), 1460-1463.

[26] N.Sloane, Tables of spherical codes (with collaboration of R.H. Hardin, W.D. Smith and others) published electronically at http://www2.research.att.com/njas/packings, 2000.

[27] E. Trefftz, Ein Gegenstück zum Ritzschen Verfahren, Sec. Inte. Cong. Appl. Mech., 1926, 131-137.

[28] N. Yi and H. Liu, An Energy Conserving Local Discontinuous Galerkin Method for a Nonlinear Variational Wave Equation, Commun. Comput. Phys., 23(2018), 747-772.

[29] L. Yuan, The plane wave methods for the time-harmonic elastic wave problems with complex valued coefficients, submitted.

[30] L. Yuan, The plane wave discontinuous Galerkin method combined with local spectral finite elements for the wave propagation in anisotropic media, Numer. Math. Theor. Meth. Appl., 2018, 10.4208/nmtma.OA-2017-0139.

[31] L. Yuan and Q. Hu, A solver for Helmholtz system generated by the discretization with wave shape functions, Adv. Appl. Math. Mech., 5(2013), 791-808.

[32] L. Yuan, Q. Hu and H. B. An, Parallel preconditioners for plane wave Helmholtz and Maxwell systems with large wave numbers, Int. J. Numer. Anal. Model., 13(2016), 802-819.

[33] L. Yuan and Q. Hu, Comparisons of three kinds of plane wave methods for the Helmholtz equation and time-harmonic Maxwell equations with complex wave numbers, J. Comput. Appl. Math., 344(2018), 323-345.

[34] L. Yuan and Q. Hu, The Plane Wave Methods Combined with Local Spectral Finite Elements for the wave propagation in Anisotropic Media, Adv. Appl. Math. Mech., 10(5), 2018, 1-32.

[35] L. Zhu and H. Wu, Preasymptotic error analysis of CIP-FEM and FEM for Helmholtz equation with large number, SIAM J. Numer. Anal., 51(2013), 1828-1852.